AD_____

Award Number: DAMD17-01-1-0317

TITLE: Functional Analysis of Interactions Between 53BP1, BRCA1 and p53

PRINCIPAL INVESTIGATOR: Irene M. Ward, Ph.D.

CONTRACTING ORGANIZATION: Mayo Clinic Rochester
Rochester, Minnesota 55905

REPORT DATE: July 2004

TYPE OF REPORT: Annual Summary

PREPARED FOR: U.S. Army Medical Research and Materiel Command
Fort Detrick, Maryland 21702-5012

DISTRIBUTION STATEMENT: Approved for Public Release;
Distribution Unlimited

REPORT DOCUMENTATION PAGE

Form Approved
OMB No. 074-0188

1. AGENCY USE ONLY (Leave blank)	2. REPORT DATE	3. REPORT TYPE AND DATES COVERED
	July 2004	Annual Summary (1 July 2001 - 30 June 2004)

4. TITLE AND SUBTITLE
Functional Analysis of Interactions Between 53BP1, BRCA1 and p53

5. FUNDING NUMBERS
DAMD17-01-1-0317

6. AUTHOR(S)
Irene M. Ward, Ph.D.

7. PERFORMING ORGANIZATION NAME(S) AND ADDRESS(ES)
Mayo Clinic Rochester
Rochester, Minnesota 55905

E-Mail: rappold.irene@mayo.edu

8. PERFORMING ORGANIZATION REPORT NUMBER

9. SPONSORING / MONITORING AGENCY NAME(S) AND ADDRESS(ES)
U.S. Army Medical Research and Materiel Command
Fort Detrick, Maryland 21702-5012

10. SPONSORING / MONITORING AGENCY REPORT NUMBER

11. SUPPLEMENTARY NOTES
Original contains color; all DTIC reproductions will be black and white.

12a. DISTRIBUTION / AVAILABILITY STATEMENT
Approved for Public Release; Distribution Unlimited

12b. DISTRIBUTION CODE

13. Abstract ***(Maximum 200 Words)*** *(abstract should contain no proprietary or confidential information)*

The ability to sense DNA damage and activate response pathways that coordinate cell cycle progression and DNA repair is essential for the maintenance of genomic integrity. Based on its conserved BRCT (BRCA1 C-terminal) domains, 53BP1 has been implicated in the DNA damage response. By studying the subcellular localization and molecular interaction of 53BP1, we could show that 53BP1 is rapidly activated in response to ionizing radiation and localizes to the sites of DNA double strand breaks. We mapped the region required for foci formation and could demonstrate that this region interacts with phoshorylated H2AX, a histone 2A variant that keeps 53BP1 in the vicinity of DNA lesions. Other interaction partners of 53BP1 include the tumor suppressor proteins p53 and BRCA1. By using a 53BP1 knock out model, we could show that 53BP1 itself acts as a tumor suppressor and that 53BP1 and p53 deficiency synergize in tumorigenesis. Furthermore, the loss of a single 53BP1 allele enhances the susceptibility to cancer in the absence of p53.

14. SUBJECT TERMS	15. NUMBER OF PAGES
DNA damage, DNA repair, tumorigenesis, genomic stability	42
	16. PRICE CODE

17. SECURITY CLASSIFICATION OF REPORT	18. SECURITY CLASSIFICATION OF THIS PAGE	19. SECURITY CLASSIFICATION OF ABSTRACT	20. LIMITATION OF ABSTRACT
Unclassified	Unclassified	Unclassified	Unlimited

Table of Contents

INTRODUCTION

The ability to sense DNA damage and activate response pathways that coordinate cell cycle progression and DNA repair is essential for the maintenance of genomic integrity. Defects in recognition and repair of DNA damage may be the decisive step in the transformation of a healthy cell into a tumor cell. 53BP1 had been suggested to participate in the DNA damage response pathway based on its C-terminal tandem BRCT (BRCA1 C-terminal) domain and the observation that 53BP1 relocalizes to discrete nuclear foci upon exposure of cells to ionizing radiation (Anderson et al., 2001; Rappold et al., 2001; Schultz et al., 2000; Xia et al., 2000). It was originally identified in a yeast two-hybrid screen as a protein that binds to the central DNA-binding domain of the tumor suppressor p53 and activates p53-dependent gene transcription (Iwabuchi et al., 1994; Iwabuchi et al., 1998). To obtain insight into the function of 53BP1 we asked whether endogenous 53BP1 interacts with p53, BRCA1 or other proteins known to be involved in the DNA damage response. Furthermore, using a 53BP1 knock out model, we investigated whether loss of 53BP1 function leads to defects in DNA repair and/or cell cycle checkpoint control and contributes to tumorigenesis.

BODY

As outlined in the *Statement of Work*, the first two years of the grant proposal focused on the interaction of 53BP1 with the tumor suppressors BRCA1 and p53. We had produced monoclonal and polyclonal antibodies towards 53BP1 and demonstrated that 53BP1 colocalizes and interacts with BRCA1 several hours after exposure of cells to IR (Fig.1).

Fig.1: Co-immunoprecipitation of 53BP1 and BRCA1 following DNA damage. K562 cells were exposed to 0 or 50 of γ-radiation 30 hours prior immunoprecipitation with affinity-purified anti-BRCA1 plyclonal antibody. The samples were processed for electrophoresis, separated on a 4-15% SDS gel and immunoblotted with anti-53BP1 prior re-blotted with anti-BRCA1 as indicated.

This interaction occurs at sites of DNA double strand breaks as shown by co-immunostaining with an antibody towards the activated form of H2AX, a histone H2A variant that becomes phosphorylated at areas of DNA stand breaks (Rappold et al., 2001, appendix). In contrast, the interaction of 53BP1 and p53 does not depend on DNA damage (Fig 2) although the stabilization of p53 in response to DNA damage or replication arrest results in an increase in the amount of 53BP1 co-immunoprecipitated by p53.

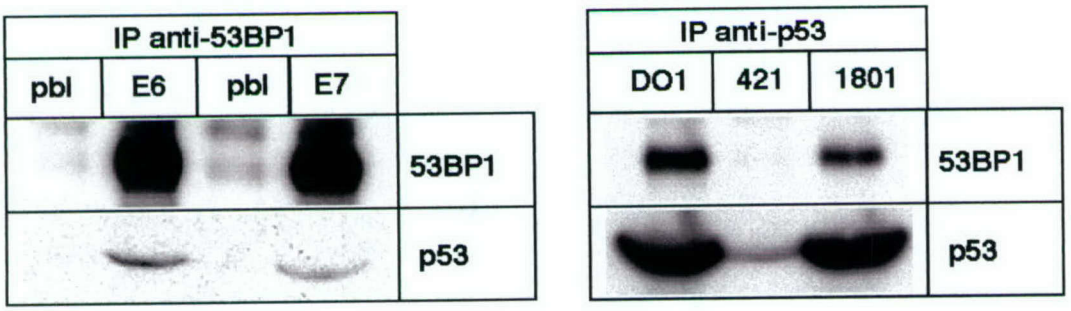

Fig,2: Co-immunoprecipitation of p53 and 53BP1. Extracts of untreated HBL100 cells were either immunoprecipitated with two different anti-53BP1 antisera (E6, E7) or with 3 different anti-p53 antibodies (DO1,421,1801) and immunoblotted with either anti-53BP1 (E7) or anti-p53 (DO1) antibody. Anti-p53 antibody 421 is raised against a mutant form of p53.

To characterize the 53BP1 domains that mediate the recruitment of 53BP1 to sites of DNA strand breaks we generated a series of HA-tagged 53BP1 full-length and deletion mutants and studied the IR-induced relocalization of these fusion proteins in transiently transfected U2OS cells. We could show that a region upstream of the tandem BRCT domains is required and sufficient for the accumulation of 53BP1 to DNA strand breaks (Ward et al., 2003a, appendix). Interestingly, this region binds to phosphorylated but not unphosphorylated H2AX *in vitro* suggesting that phosphorylated H2AX keeps 53BP1 in the vicinity of DNA lesions (Ward et al., 2003a, appendix).

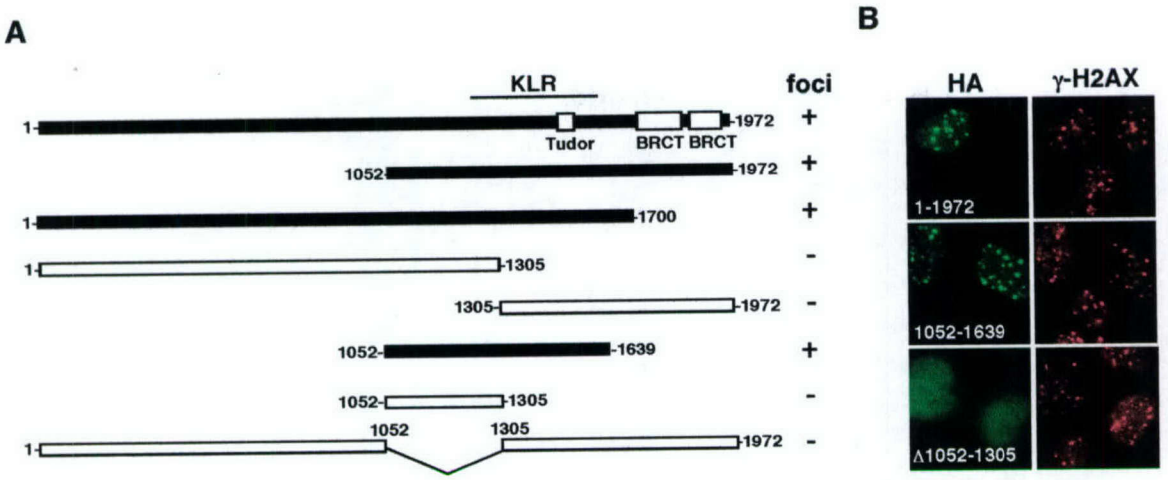

Fig.3: A region upstream of the BRCT domains is required and sufficient for damage-induced focus localization of 53BP1. **A**: Schematic diagram of the wild-type or mutant 53BP1 constructs that were N-terminally fused to a 3xNLS and an HA-tag. Their ability to form damage-induced foci is indicated by a (+). KLR refers to the kinetochore localization region. **B**: U20S cells transiently expressing the HA-53BP1 constructs were irradiated with 1 Gy and immunostained 1 h later with anti- HA and anti-γ-H2AX antibodies.

Since 53BP1 becomes hyperphosphorylated in response to DNA damage, we wondered whether 53BP1 phosphorylation is required for the interaction with phospho-H2AX. We mapped four *in vitro* phosphorylation sites, raised phospho-specific antibodies against these sites and showed that at least two of them (S25 and S29) are phosphorylated *in vivo* by ATM, the kinase mutated in cancer prone ataxia telangiectasia patients. 53BP1 mutants that lack all four phosphorylation sites were still able to relocate to γ-H2AX containing foci in response to ionizing radiation, suggesting that 53BP1 phosphorylation is not required for 53BP1 accumulation. In addition, 53BP1 mutants that lack the region required for 53BP1 accumulation and do not relocate to foci in response to ionizing radiation can still be phosphorylated (Ward et al., 2003a, appendix). Therefore, 53BP1 phosphorylation and 53BP1 relocalization appear to be regulated independently.

To examine the pysiological relevance of the observed interactions between 53BP1, BRCA1 and p53 we generated a 53BP1-deficient mouse model (Ward et al., 2003b, appendix). Mice that lack 53BP1 were growth retarded, radiation sensitive and immunodeficient (Ward et al., 2003b, apendix). Immunofluorescence staining of BRCA1 on mouse embryonic fibroblasts (MEFs) derived from 53BP1-/- and 53BP1+/+

littermates demonstrated that 53BP1 is not required for radiation-induced relocation of BRCA1 to DNA strand breaks.

To check whether 53BP1 transduces a DNA damage signal to p53, we compared irradiation-induced p53 stabilization in 53BP1+/+ and 53BP1-/- thymocytes and MEFs. Although p53 levels increased in both 53BP1 wild-type and 53BP1-deficient cells upon irradiation, in some experiments we observed a reduced and/or delayed p53 response in the absence of 53BP1 suggesting that 53BP1 may have some effect on p53 regulation (Fig. 4).

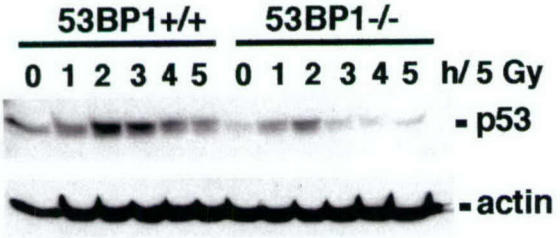

Fig 4: Reduced p53 response in irradiated 53BP1-deficient embryonic cells. 53BP1 wild-type or deficient cells were either mock treated or irradiated with 5 Gy. At the indicated time points p53 levels were analyzed by Western blotting. B-actin was used as a loading control.

In addition, 53BP1 appears to be required for efficient accumulation of p53 and BLM at the sites of stalled replication and DNA strand breaks (Fig.5)(Sengupta et al., 2004). BLM is the protein mutated in patients with Boom's syndrome, a rare genetic disorder characterized by chromosomal aberrations, genetic instability and cancer predisposition.

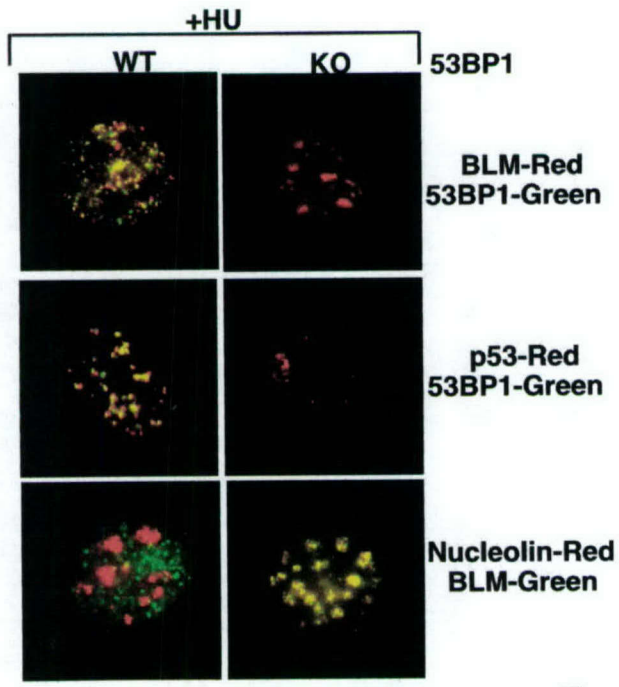

Fig. 5: Lack of 53BP1 prevents the efficient accumulation of BLM and p53 at the sites of stalled DNA replication forks. 53BP1 wild-type or deficient mice were treated with hydroxyurea (HU) for 6h prior immunostaining with antibodies against BLM, 53BP1 p53 and nucleolin as indicated

To explore whether 53BP1 is involved n the maintenance of genomic stability we looked for chromosomal aberrations in 53BP1-deficient MEFs. 53BP1-/- cells showed a tendency to aneuploidy and tetraploidy when compared to 53BP1 wild-type cells. Genomic instability is a hallmark and prerequisite of cancer. Notably, about 8% of the 53BP1-deficient mice developed thymic lymphomas within 4 and 7 months of age (Fig.6). In contrast, none of the 53BP1+/+ and 53BP1+/- littermates developed any tumors within the first year of life (Ward et al., 2003b, appendix).

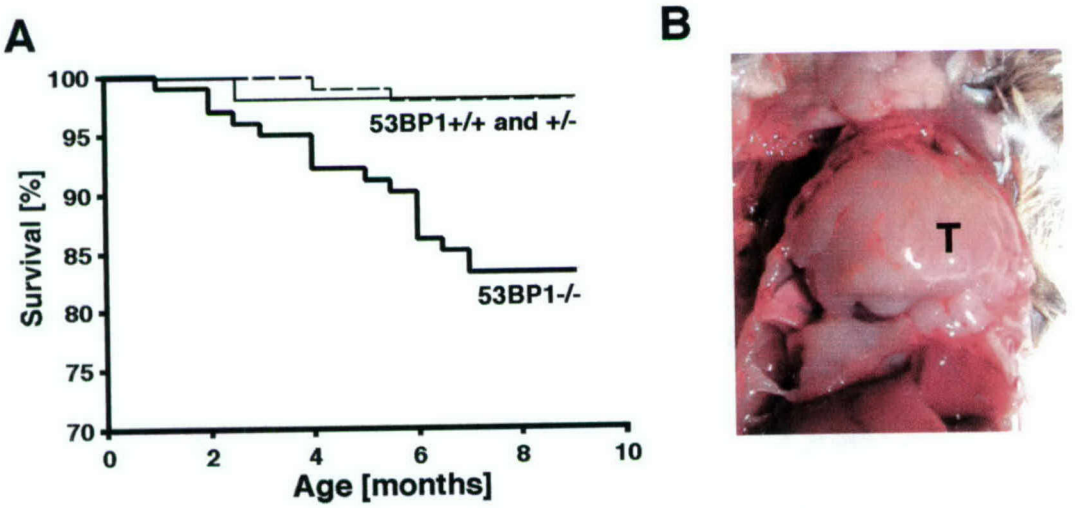

Fig. 6: 53BP1 -/-mice show increased incidence of spontaneous tumors. **A**: Overall survival of 53BP1+/+ (n=54), 53BP1+/- (n=97) and 53BP1-/- (n=101) over the course of 10 months. **B**: Massive thymic lymphoma (T) in a 4-months old 53BP1-/- mouse.

Since the genetic background of a given mouse strain greatly influences tumor susceptibility as well as tumor type we back-crossed our 53BP1-deficient mice into a BALB/c background. We are especially interested to examine whether 53BP1-deficient mice will develop a higher incidence of breast and/or ovarian cancers when compared to 53BP1 wild-type mice. In addition, we crossed 53BP1 heterozygous mice with p53 heterozygous mice of the same mixed background to investigate how both proteins contribute to tumor formation. Our results indicate that p53-/-53BP1-/- double knock out animals die much earlier than p53-/- 53BP1+/+ mice suggesting that 53BP1 and p53 synergize in tumorigenesis. Moreover, 53BP1 haplosufficiency also significantly

accelerates tumor development, an observation that emphasizes the role of 53BP1 in tumor suppression (Fig.7).

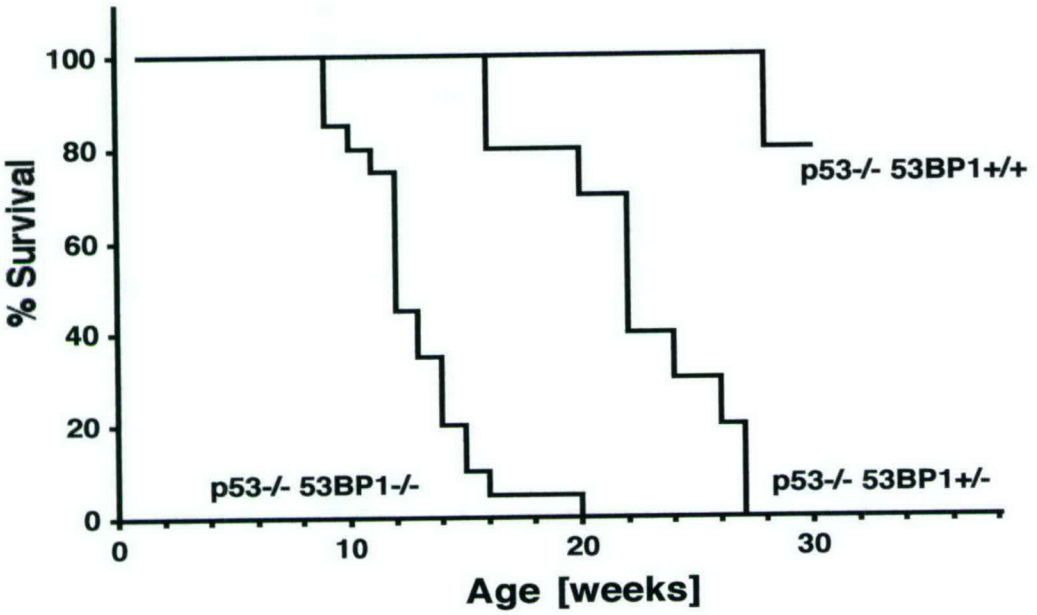

Fig.7: 53BP1 and p53 deficiency synergize in tumorigenesis. Survival curves for p53-/-53BP1+/+, p53-/-53BP1+/- and p53-/-53BP1+/+ mice plottes as a function of time in weeks.

To investigate whether 53BP1 mutations contribute to the development of breast cancer (Task 3), Dr. Fergus Couch at the Mayo Clinic Rochester screened several breast cancer samples for mutations in the BRCT domain of 53BP1. Our original assumption was that the BRCT domains of 53BP1 are of similar functional importance as the BRCT domains in BRCA1. However, none of the samples tested showed any mutations within this C-terminal region.

We also looked at 53BP1 expression in breast cancer tissue and found that 53BP1 is over-expressed in a number of breast cancers (Fig.8). However, there was no correlation between 53BP1 expression and tumor grade or outcome. Moreover, 53BP1 expression did not correlate with p53 expression in these tissues (Fig. 8).

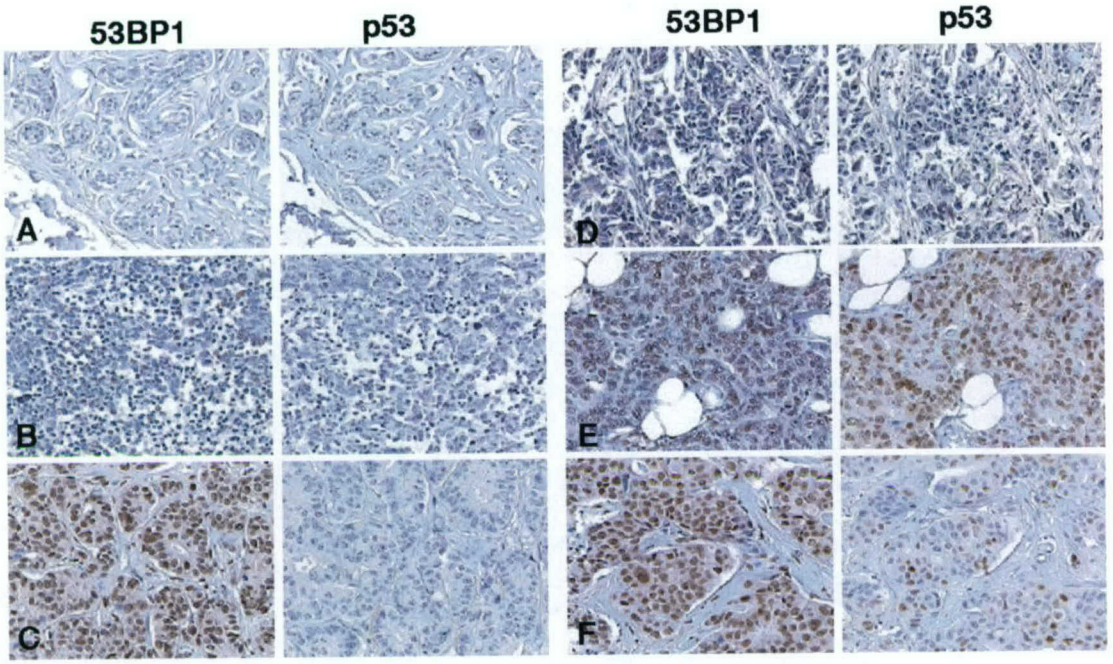

Fig. 8: 53BP1 and p53 expression in breast cancer tissue analyzed by immunohistochemistry. A: Normal breast, B-C: Medullary Carcinoma, D-F: Invasive Ductal Carcinoma.

To investigate whether the tumor suppressor function of 53BP1 is due to a role of 53BP1 in DNA repair, we analyzed the proficiency of DNA double strand (DSB) repair in 53BP1-deficient cells. Our findings showed that homologous recombination repair is not impaired in the absence of 53BP1. Similarly, the non-homologous joining of RAG-induced DSBs during the process of V(D)J recombination does not require 53BP1. However, class switch recombination (CSR) was severely impaired in 53BP1-deficient mice suggesting that the joining of AID-induced breaks in stimulated lymphocytes requires 53BP1 (Fig. 10, and (Ward et al., 2004, appendix).

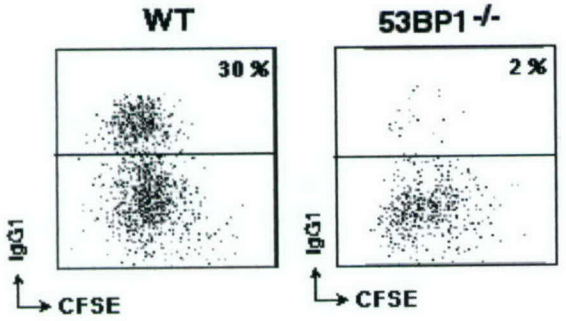

Fig.9: Impaired CSR in the absence of 53BP1. Cell division and surface IgG1 expression were measured by flow cytometry on live CFSE-labeled wild type (WT) and 53BP1$^{-/-}$ B cells. stimulated with LPS plus IL-4 for 4 days.

KEY RESEARCH ACCOMPLISHMENTS

We have shown that:

- 53BP1 participates together with BRCA1 and p53 in the DNA damage response
- 53BP1 rapidly accumulates at sites of DNA strand breaks in response to IR
- 53BP1 accumulation is mediated by a direct interaction with phospho-H2AX
- 53BP1-deficient mice are radiation sensitive, growth retarded and immunodeficient
- 53BP1-deficient mice have a higher incidence of developing tumors
- 53BP1 and p53 deficiency synergize in tumorigenesis
- 53BP1 haploinsufficiency enhances susceptibility to cancer in the absence of p53
- 53BP1 is overexpressed in a subset of breast cancer tissues
- 53BP1 is required for the endjoining of DSBs during CSR

REPORTABLE OUTCOMES

Manuscripts:

Rappold, I.M., Iwabuchi, K., Date, T. and Chen, J. (2001) Tumor suppressor p53 binding protein 1 (53BP1) is involved in DNA damage-signaling pathways. *J Cell Biol*, **153**,

Ward, I.M., Wu, X. and Chen, J. (2001) Threonine 68 of Chk2 is phosphorylated at sites of DNA strand breaks. *J Biol Chem*, **276**, 47755-8)

Ward, I.M. and Chen, J. (2001) Histone H2AX is phosphorylated in an ATR-dependent manner in response to replicational stress. *J Biol Chem*, **276**, 47759-62.

Fernandez-Capetillo, O., Chen, H.T., Celeste, A., **Ward, IM.**, Romanienko, P.J., Morales, J.C., Naka, K., Xia, Z., Camerini-Otero, R.D., Motoyama, N., Carpenter, P.B., Bonner, W.M., Chen, J. and Nussenzweig, A. (2002) DNA damage-induced G2-M checkpoint activation by histone H2AX and 53BP1. *Nat Cell Biol*, **4**, 993.

Ward, I.M., Minn, K., Jorda, K.G. and Chen, J. (2003a) Accumulation of checkpoint protein 53BP1 at DNA breaks involves its binding to phosphorylated histone H2AX. *J Biol Chem*, **278**, 19579-82.

Ward, I.M., Minn, K., van Deursen, J. and Chen, J. (2003b) p53 Binding protein 53BP1 is required for DNA damage responses and tumor suppression in mice. *Mol Cell Biol*, **23**, 2556-63.

Ward IM, Reina-San-Martin B, Olaru A, Minn K, Tamada K, Lau JS, Cascalho M, Chen L, Nussenzweig A, Livak F, Nussenzweig MC, Chen J (2004) 53BP1 is required for class switch recombination. J Cell Biol. 165(4):459-64.

Ward IM, Minn K, Chen J. (2004) UV-induced ataxia-telangiectasia-mutated and Rad3-related (ATR) activation requires replication stress. J Biol Chem 12;279(11):9677-80.

Ward IM, Chen J. Early events in DNA damage response. Review.(2004) Current Topics in Developmental Biology in press.

Sengupta S., Robles AI, Linke SP, Sinogeeva N, Zhang, R, Pedeux R, **Ward IM**, Celeste A, Nussenzweig A, Chen J, Halazonetis T, Harris CC (2004) Functional

interaction between BLM helicase and 53BP1 in a chk1-mediated pathway during S-phase arrest. JCB in press

Animal model:

Generation of a 53BP1-deficient mouse model

Development of cell lines:

Establishment of immortal 53BP1-deficient and 53BP1-wildtype mouse embryonic cell lines

CONCLUSIONS

Our data demonstrate that 53BP1 plays a role early in the DNA damage response. Upon exposure of cells to ionizing radiation, 53BP1 relocalizes to sites of DNA double strand breaks and accumulates there by binding to phosphorylated histone H2AX. The region that binds to phosphorylated H2AX resides within the region required for 53BP1 foci formation upstream of the C-terminal BRCT domains. Moreover, 53BP1 becomes hyperphosphorylated by ATM in response to ionizing radiation although phosphorylation can occur in the absence of 53BP1 foci formation suggesting that both events are regulated independently. Knock out mice that lack 53BP1 protein exhibit an increased sensitivity to ionizing radiation and show an increased incidence of developing lymphomas. Furthermore, 53BP1 and p53 deficiency synergize in tumorigenesis and the loss of a single 53BP1 allele enhances the susceptibility to cancer in the absence of p53. Although 53BP1 appears not to be required for the gross repair of DNA DSBs, some breaks like the ones generated during class switch recombination cannot effectively be joined in the absence of 53BP1. It is therefore reasonable to speculate that 53BP1 deficiency impairs the repair of certain DSBs thus initiating translocations that can lead to oncogenic gene amplification and transformation.

REFERENCES

Anderson, L., C. Henderson, and Y. Adachi. 2001. Phosphorylation and rapid relocalization of 53BP1 to nuclear foci upon DNA damage. *Mol Cell Biol.* 21:1719-29.

Iwabuchi, K., P.L. Bartel, B. Li, R. Marraccino, and S. Fields. 1994. Two cellular proteins that bind to wild-type but not mutant p53. *Proc Natl Acad Sci U S A.* 91:6098-102.

Iwabuchi, K., B. Li, H.F. Massa, B.J. Trask, T. Date, and S. Fields. 1998. Stimulation of p53-mediated transcriptional activation by the p53-binding proteins, 53BP1 and 53BP2. *J Biol Chem.* 273:26061-8.

Rappold, I., K. Iwabuchi, T. Date, and J. Chen. 2001. Tumor Suppressor p53 Binding Protein 1 (53BP1) Is Involved in DNA Damage-signaling Pathways. *J Cell Biol.* 153:613-20.

Schultz, L.B., N.H. Chehab, A. Malikzay, and T.D. Halazonetis. 2000. p53 Binding Protein 1 (53BP1) Is an Early Participant in the Cellular Response to DNA Double-Strand Breaks. *J Cell Biol.* 151:1381-1390.

Ward, I.M., K. Minn, K.G. Jorda, and J. Chen. 2003a. Accumulation of checkpoint protein 53BP1 at DNA breaks involves its binding to phosphorylated histone H2AX. *J Biol Chem.* 278:19579-82.

Ward, I.M., K. Minn, J. Van Deursen, and J. Chen. 2003b. p53 Binding Protein 53BP1 Is Required for DNA Damage Responses and Tumor Suppression in Mice. *Mol Cell Biol.* 23:2556-63.

Ward, I.M., B. Reina-San-Martin, A. Olaru, K. Minn, K. Tamada, J.S. Lau, M. Cascalho, L. Chen, A. Nussenzweig, F. Livak, M.C. Nussenzweig, and J. Chen. 2004. 53BP1 is required for class switch recombination. *J Cell Biol* 165:459-464.

UV-induced ataxia-telangiectasia-mutated and Rad3-related (ATR) activation requires replication stress. *J Cell Biol.* 165:459-64.

Xia, Z., J.C. Morales, W.G. Dunphy, and P.B. Carpenter. 2000. Negative cell cycle regulation and DNA-damage inducible phosphorylation of the BRCT protein 53BP1. *J Biol Chem.*

APPENDICES

Rappold, I., K. Iwabuchi, T. Date, and J. Chen. (2001). Tumor Suppressor p53 Binding Protein 1 (53BP1) Is Involved in DNA Damage-signaling Pathways. *J Cell Biol.* 153:613-20.

Ward, I.M., Minn, K., Jorda, K.G. and Chen, J. (2003a) Accumulation of checkpoint protein 53BP1 at DNA breaks involves its binding to phosphorylated histone H2AX. *J Biol Chem*, **278**, 19579-82.

Ward, I.M., Minn, K., van Deursen, J. and Chen, J. (2003b) p53 Binding protein 53BP1 is required for DNA damage responses and tumor suppression in mice. *Mol Cell Biol*, **23**, 2556-63.

Ward, I.M., B. Reina-San-Martin, A. Olaru, K. Minn, K. Tamada, J.S. Lau, M. Cascalho, L. Chen, A. Nussenzweig, F. Livak, M.C. Nussenzweig, and J. Chen (2004). 53BP1 is required for class switch recombination. *J Cell Biol* 165:459-464.

JCB Report

Tumor Suppressor p53 Binding Protein 1 (53BP1) Is Involved in DNA Damage–signaling Pathways

Irene Rappold,* Kuniyoshi Iwabuchi,* Takayasu Date,‡ and Junjie Chen*

*Division of Oncology Research, Mayo Clinic, Rochester, Minnesota 55905; and ‡Department of Biochemistry, Kanazawa Medical University, Ishikawa 920-0293, Japan

Abstract. The tumor suppressor p53 binding protein 1 (53BP1) binds to the DNA-binding domain of p53 and enhances p53-mediated transcriptional activation. 53BP1 contains two breast cancer susceptibility gene 1 COOH terminus (BRCT) motifs, which are present in several proteins involved in DNA repair and/or DNA damage–signaling pathways. Thus, we investigated the potential role of 53BP1 in DNA damage–signaling pathways. Here, we report that 53BP1 becomes hyperphosphorylated and forms discrete nuclear foci in response to DNA damage. These foci colocalize at all time points with phosphorylated H2AX (γ-H2AX), which has been previously demonstrated to localize at sites of DNA strand breaks. 53BP1 foci formation is not restricted to γ-radiation but is also detected in response to UV radiation as well as hydroxyurea, camptothecin, etoposide, and methylmethanesulfonate treatment. Several observations suggest that 53BP1 is regulated by ataxia telangiectasia mutated (ATM) after DNA damage. First, ATM-deficient cells show no 53BP1 hyperphosphorylation and reduced 53BP1 foci formation in response to γ-radiation compared with cells expressing wild-type ATM. Second, wortmannin treatment strongly inhibits γ-radiation–induced hyperphosphorylation and foci formation of 53BP1. Third, 53BP1 is readily phosphorylated by ATM in vitro. Taken together, these results suggest that 53BP1 is an ATM substrate that is involved early in the DNA damage–signaling pathways in mammalian cells.

Key words: 53BP1 • DNA damage • nuclear foci • γ-H2AX • ATM

Introduction

Cells have evolved various sophisticated pathways to sense and overcome DNA damage as a mechanism to preserve the integrity of the genome. Environmental attacks like radiation or toxins, as well as spontaneous DNA lesions, trigger checkpoint activation and consequent cell cycle arrest and/or apoptosis. One key protein that coordinates DNA repair with cell cycle progression and apoptosis is the tumor suppressor protein p53. P53 is activated and posttranslationally modified in response to DNA damage (Appella and Anderson, 2000). These modifications include phosphorylation by ataxia telangiectasia mutated (ATM),[1] a protein kinase implicated in DNA damage–signaling pathways (Canman et al., 1998; Khanna et al., 1998). By transcriptionally activating genes involved in cell cycle control, DNA repair, and apoptosis, p53 participates in the maintenance of the genomic integrity after DNA damage.

P53 interacts with p53 binding protein 1 (53BP1). 53BP1 has been identified in a yeast two hybrid screen as a protein that interacts with the central DNA–binding domain of p53 (Iwabuchi et al., 1994). Similar to breast cancer susceptibility gene 1 (BRCA1; Ouchi et al., 1998; Zhang et al., 1998a; Chai et al., 1999), 53BP1 enhances p53-dependent transcription (Iwabuchi et al., 1998). Interestingly, the COOH terminus of 53BP1 contains tandem BRCA1 COOH terminus (BRCT) motifs. This motif was first identified in the COOH-terminal region of BRCA1 and has since been found in a large number of proteins involved in various aspects of cell cycle control, recombination, and DNA repair in mammals and yeast (Koonin et al., 1996; Bork et al., 1997; Callebaut and Mornon, 1997). The func-

Address correspondence to Junjie Chen, Guggenheim 1306, Division of Oncology Research, Mayo Clinic, 200 First Street, S.W., Rochester, MN 55905. Tel.: (507) 538-1545. Fax: (507) 284-3906. E-mail: chen.junjie@mayo.edu

[1]*Abbreviations used in this paper:* ATM, ataxia telangiectasia mutated; BRCA1, breast cancer susceptibility gene 1; BRCT, BRCA1 COOH terminus; DNA-PK, DNA-dependent protein kinase; 53BP1, binding protein 1; GST, glutathione *S*-transferase; PI3K, phosphatidylinositol 3–kinase.

tion of the BRCT domain is not known. However, evidence suggests that BRCT domains may mediate protein–protein interactions (Zhang et al., 1998b).

The presence of BRCT domains in 53BP1 and the reported interaction with p53 prompted us to investigate whether 53BP1 is involved in DNA damage–response pathways. Here we report that 53BP1 becomes hyperphosphorylated and rapidly relocates to the sites of DNA strand breaks in response to ionizing radiation. 53BP1 foci formation is reduced in ATM-deficient cells and can be inhibited by wortmannin in ATM wild-type cells. Moreover, radiation-induced hyperphosphorylation of 53BP1 is absent in cells treated with wortmannin, as well as in ATM-deficient cells. Taken together, these results strongly suggest that 53BP1 participates in DNA damage–signaling pathways and is regulated by ATM after γ-radiation.

Materials and Methods

Cell Culture and Treatments with DNA-damaging Agents

Cells were grown in RPMI 1640 medium supplemented with 10% fetal bovine serum at 37°C with 5% CO_2. FT169A and YZ5 cells were provided by Dr. Y. Shilon (Tel Aviv University, Ramat Aviv, Israel). Cells grown on coverslips were irradiated in a JL Shepherd ^{137}Cs radiation source at a rate of 1 Gy/min for doses of 1–5 Gy or 10 Gy/min for a dose of 10 Gy. UV light was delivered in a single pulse (50 J/m^2) using a Stratalinker UV source (Stratagene). Before UV irradiation, the culture medium was removed and the medium was replaced immediately after irradiation. All cells were returned to the incubator for recovery and harvested at the indicated times. Genotoxic agents and other drugs were used at the indicated concentrations. After a 1-h exposure, the cells were harvested for immunostaining.

Immunoprecipitation, Immunoblotting, and Immunostaining

Immunoprecipitation, immunoblotting, and immunostaining were performed as described previously (Scully et al., 1997). Rabbit polyclonal anti-53BP1 serum E7 was raised against a glutathione *S*-transferase (GST) fusion protein encoding residues 338–671 of 53BP1. Mouse anti-53BP1 monoclonal antibodies were raised against a mix of three GST fusion proteins encoding residues 1–337, 338–671, and 1,331–1,664, respectively, of 53BP1. Antiphospho-H2AX antibody was generated as described previously (Rogakou et al., 1999).

ATM Kinase Assay

ATM was immunoprecipitated from K562 cells using anti-ATM antibody Ab3 (Oncogene Research Products). Aliquots of the ATM–protein A Sepharose immunocomplexes were resuspended in 25 μl kinase buffer (10 mM Hepes, pH 7.4, 50 mM NaCl, 10 mM $MgCl_2$, 10 mM $MnCl_2$, 1 mM DTT, 10 nM ATP) and incubated for 20 min at 30°C with 10 μCi of [γ^{32}]P-ATP and 1 μg of various affinity-purified GST fusion proteins containing different fragments of 53BP1.

Results

53BP1 Forms Nuclear Foci in Response to Various Types of DNA Damage

Several proteins, including BRCA1 and Mre11/Rad50/Nbs1, form DNA damage–regulated, subnuclear foci in the cell. To determine whether 53BP1 participates in DNA damage–signaling pathways, we examined 53BP1 localization after various types of DNA damage using several anti-53BP1 polyclonal and monoclonal antibodies generated for this study. All antibodies specifically recognize endogenous, as well as HA-tagged, full-length 53BP1 as examined by Western blotting, immunoprecipitation, and immunostaining (data not shown). As shown in Fig. 1, 53BP1 is diffusely localized in the nuclei of normal cells, but relocates to discrete subnuclear foci structures in response to ionizing radiation (e.g., 1 Gy). These 53BP1 foci can be detected as early as 5 min after irradiation (data not shown). Higher doses of radiation (e.g., 10 Gy) lead to more but smaller 53BP1 foci (Fig. 1). The number of foci reaches a peak at ~30 min after radiation. Thereafter, the foci number slowly decreases, whereas the foci size increases (data not shown).

Foci formation is also observed in response to other DNA-damaging events. UV radiation induced the formation of numerous small foci, similar to that induced by 4NQO (a UV-mimetic agent) and hydroxyurea (Fig. 1). Treatment with the DNA topoisomerase I poison camptothecin or the topoisomerase II poison etoposide (VP16), which cause DNA single strand and double strand breaks, respectively, also resulted in the formation of 53BP1 foci. Similar results were obtained with the alkylating agent methylmethanesulfonate. However, cisplatin, a DNA cross-linking agent, induced only a few 53BP1 foci during the first hour after drug application, whereas the protein kinase inhibitor UCN-01 and the antimitotic agent paclitaxel (Taxol; Bristol-Meyers Squibb Co.) did not induce 53BP1 foci formation. Thus, different types of DNA damage trigger the recruitment of 53BP1 into discrete nuclear foci.

53BP1 Colocalizes with γ-H2AX in Response to DNA Damage

The time course of 53BP1 foci formation and disappearance is very similar to that recently described for phosphorylated H2AX (Rogakou et al., 1999; Paull et al., 2000). H2AX is one of the histone H2A molecules in mammalian cells and becomes rapidly phosphorylated after exposure of cells to ionizing radiation (Rogakou et al., 1999; Paull et al., 2000). Phosphorylated H2AX (γ-H2AX) appears within 1–3 min as discrete nuclear foci on sites of DNA double strand breaks (Rogakou et al., 1999). Similar to γ-H2AX (Rogakou et al., 1999), the number of 53BP1 foci showed a linear relationship with the severity of DNA damage (Fig. 1 and data not shown). As shown in Fig. 2 A, damage-induced 53BP1 foci colocalized with γ-H2AX at the various time points analyzed. The number of 53BP1 foci was identical to that of γ-H2AX throughout the course of the experiment. In addition, coimmunoprecipitation analysis revealed that 53BP1 and γ-H2AX biochemically interact after γ-radiation (Fig. 2 B). Small amounts of 53BP1 were detected in γ-H2AX immunoprecipitates prepared from irradiated HBL100 cells. In unirradiated cells, H2AX was not phosphorylated and anti–γ-H2AX antibodies did not immunoprecipitate any phosphorylated H2AX. Similarly, 53BP1 was also not present in anti–γ-H2AX immunoprecipitates prepared from unirradiated cells. These results demonstrate that 53BP1 colocalizes and interacts with γ-H2AX at the sites of DNA strand breaks after γ-radiation.

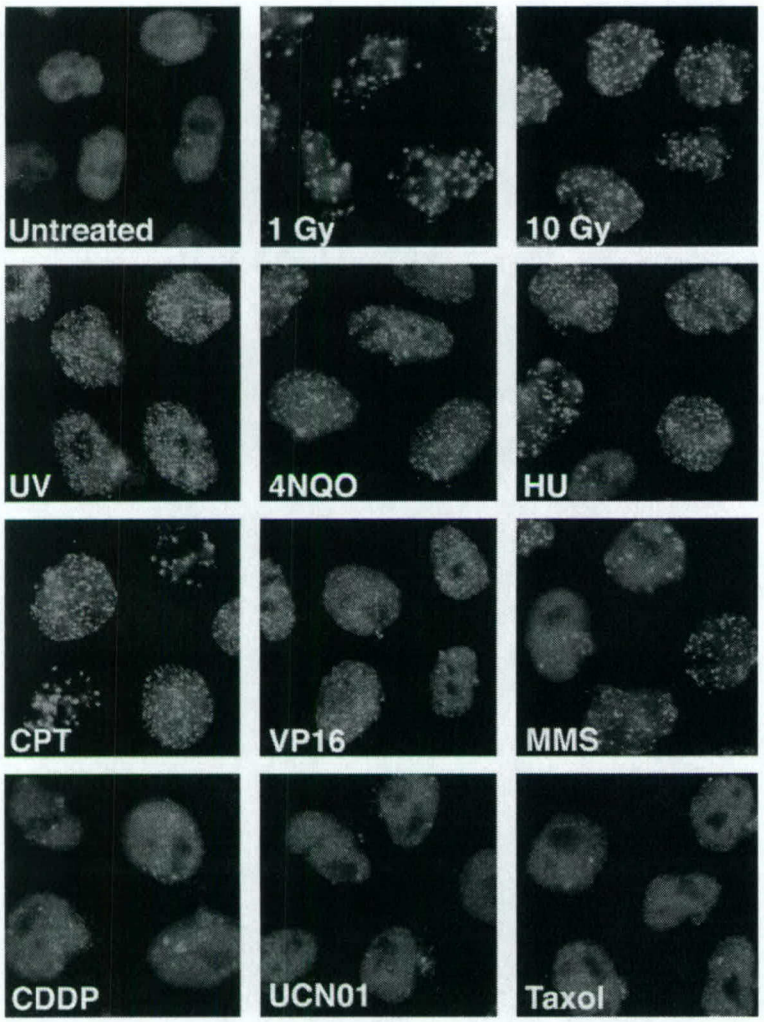

Figure 1. 53BP1 forms nuclear foci in response to DNA damage. HeLa cells were exposed to γ-irradiation (1 and 10 Gy) or a 50 J/m^2 UV pulse 1 h before immunostaining with anti-53BP1 mAb BP13. Alternatively, cells were treated for 1 h with the following drugs: 2 μg/ml 4-nitroquinoline 1-oxide (4NQO), 1 mM hydroxyurea (HU), 1 μM camptothecin (CPT), 40 μg/ml etoposide (VP16), 0.01% methylmethanesulfonate (MMS), 40 μM cisplatin (CDDP), 1 μM 7-hydroxystaurosporine (UCN-01), and 1 μM paclitaxel (Taxol).

ATM Is Involved in 53BP1 Foci Formation

Several phosphatidylinositol 3–kinase (PI3K)-related kinases, including DNA-dependent protein kinase (DNA-PK), ATM, and ATM-related kinase (ATR), participate in DNA damage–responsive pathways (Smith and Jackson, 1999; Khanna, 2000). It is possible that DNA damage–induced 53BP1 foci formation may depend on one or more of these PI3K-like kinase family members.

We first examined 53BP1 foci formation in the presence or absence of DNA-PK using two derivatives of the human glioma cell line MO59 (Lees-Miller et al., 1995). No difference in the time course of 53BP1 foci appearance and disappearance was observed in these two cell lines after exposure to 1 Gy of γ-radiation (data not shown). However, comparison was hampered by the high number of 53BP1 foci in unirradiated MO59K and MO59J cells and subtle differences might be overlooked.

We then examined whether the 53BP1 response to ionizing radiation is affected in cells lacking ATM. Immortalized ATM-deficient fibroblasts (FT169A) were compared with their isogenic derivative cells, YZ5, that have been reconstituted with wild-type ATM cDNA (Ziv et al., 1997). As shown in Fig. 3 A, although irradiation with 1 Gy resulted in a rapid formation of 53BP1 foci in the ATM-reconstituted cells (ATM+), a reduced response was observed in the cells lacking wild-type ATM (ATM−). Similar results were obtained when we compared other ATM-deficient fibroblast lines (GM03189D and GM05849C) with wild-type ATM cell lines (GM02184D and GM00637H) (Fig. 3 A). The time course of the number of 53BP1 foci per cell, as calculated from three independent experiments using YZ5 versus parental FT169A cells, is illustrated in Fig. 3 B.

To further corroborate the role of ATM in 53BP1 foci formation, we pretreated HeLa cells for 30 min with wortmannin before exposure to 1 Gy of irradiation. Wortmannin is a potent inhibitor of the PI3K-related kinases, including ATM and DNA-PK (Sarkaria et al., 1998). As shown in Fig. 3 C, pretreatment with 50 μM wortmannin greatly reduced the number of 53BP1 foci evident 1 h after γ-radiation. At an even higher dose (200 μM), wortmannin completely blocked 53BP1 foci formation. These results suggest that the kinase activities of ATM or other PI3K-related kinases are required for 53BP1 foci formation.

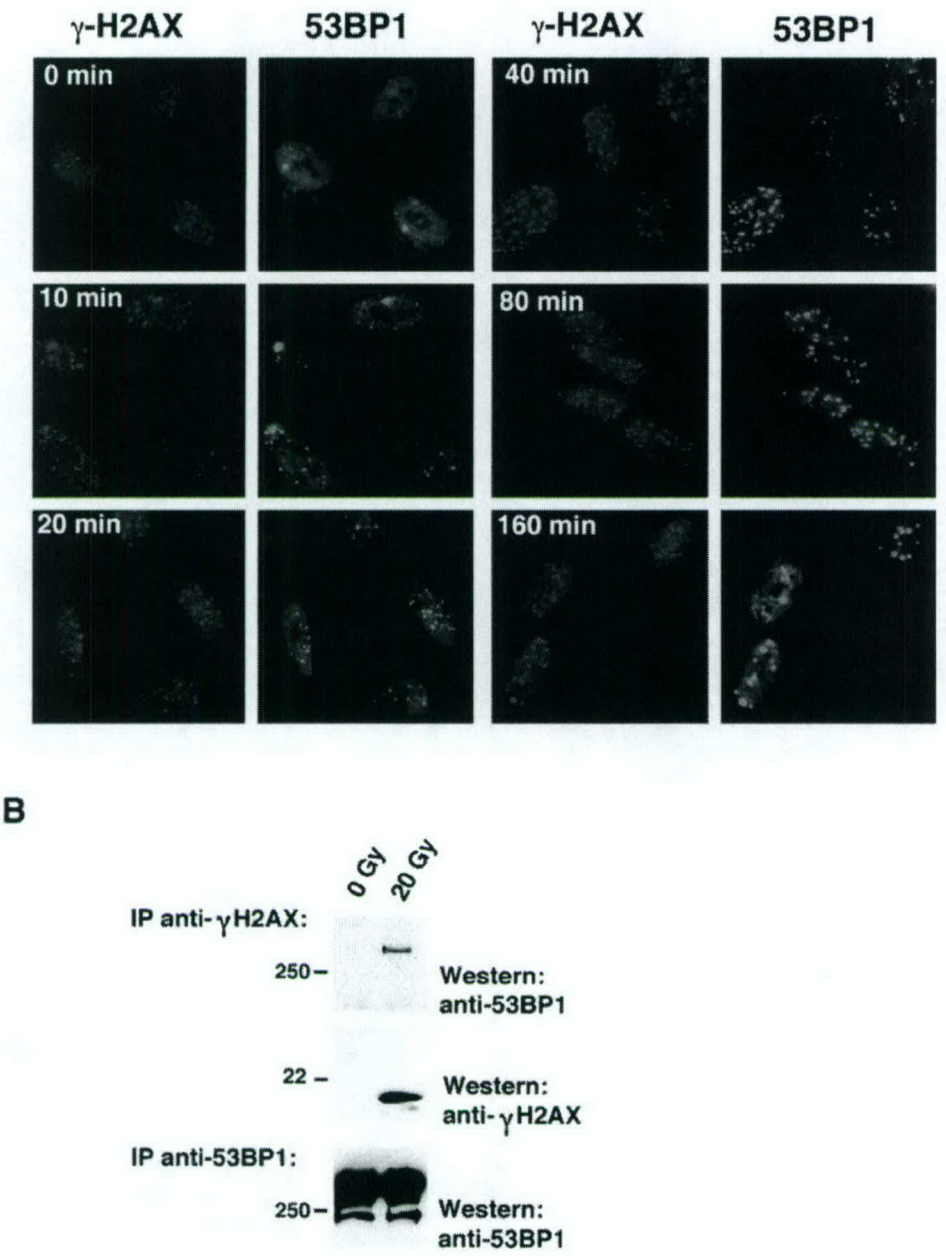

Figure 2. (A) 53BP1 colocalizes with γ-H2AX in response to γ-radiation. WI38 cells were coimmunostained with anti-53BP1 antibody BP13 and affinity-purified anti–γ-H2AX serum before (0 min) and at the indicated time points after exposure to 1 Gy (10–160 min). (B) Coimmunoprecipitation of 53BP1 and γ-H2AX after DNA damage. HBL100 cells were exposed to 0 or 20 of Gy γ-radiation 1 h before lysis in NETN buffer (150 mM NaCl, 1 mM EDTA, 20 mM Tris, pH 8, 0.5% NP-40) including 0.3 M NaCl. Immunoprecipitation experiments were performed using anti-γH2AX or anti-53BP1 antibodies. A fivefold higher amount of cell lysate was used for anti–γ-H2AX immunoprecipitation than that used for anti-53BP1 immunoprecipitation. The samples were separated on 4–15% SDS-PAGE and Western blotting was performed using either anti–γ-H2AX or anti-53BP1 antibodies as indicated.

ATM Is Required for DNA Damage-induced Hyperphosphorylation of 53BP1

Many proteins involved in DNA damage–response and/or DNA repair are phosphorylated upon DNA damage. To examine whether 53BP1 becomes phosphorylated in response to γ-radiation, K562 cells were irradiated (20 Gy) and harvested 1 h later. After immunoprecipitation using anti-53BP1 antisera, the samples were incubated for 1 h at 30°C in the presence or absence of λ protein phosphatase and separated on a 3–8% gradient SDS gel. Phosphatase treatment of unirradiated K562 cells revealed a faster migrating form of 53BP1 (Fig. 4 A). This indicates that 53BP1 is modified by phosphorylation in normal undamaged cells. Upon γ-radiation, 53BP1 showed an even slower mobility that was reversed by phosphatase treatment (Fig. 4 A). These results suggest that 53BP1 is phosphorylated in undamaged cells and becomes hyperphosphorylated after γ-radiation.

Since 53BP1 is hyperphosphorylated after γ-radiation, we then examined whether wortmannin would affect radiation-induced 53BP1 phosphorylation. As illustrated in Fig. 4 B, there was no detectable radiation-induced 53BP1 mobility shift in wortmannin (50 μM)-pretreated cells. In contrast, the radiation-induced 53BP1 mobility shift was

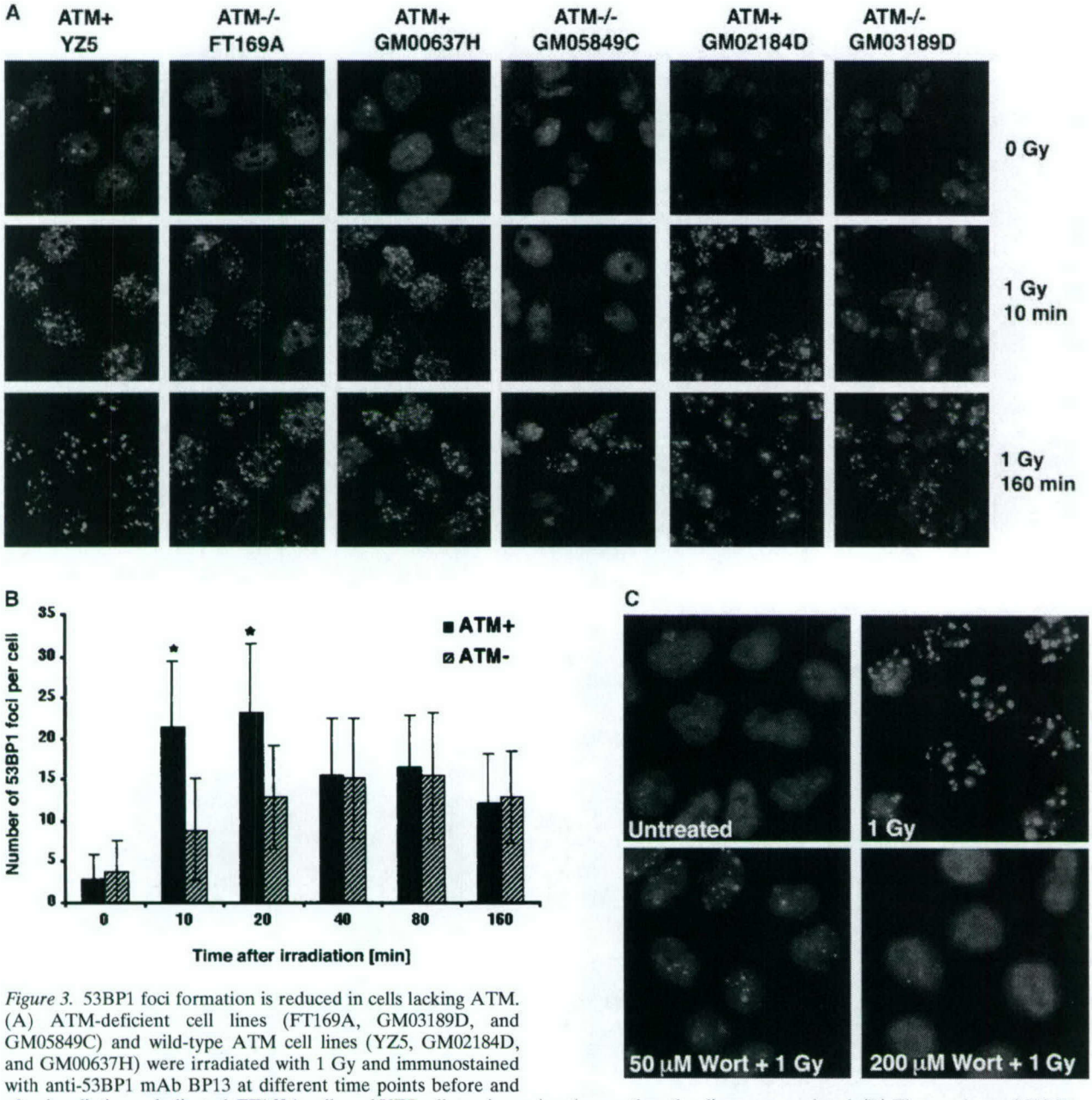

Figure 3. 53BP1 foci formation is reduced in cells lacking ATM. (A) ATM-deficient cell lines (FT169A, GM03189D, and GM05849C) and wild-type ATM cell lines (YZ5, GM02184D, and GM00637H) were irradiated with 1 Gy and immunostained with anti-53BP1 mAb BP13 at different time points before and after irradiation as indicated. FT169A cells and YZ5 cells are isogenic, whereas the other lines are unrelated. (B) The numbers of 53BP1 foci in at least 75 FT169A (ATM−) and YZ5 (ATM+) cells were counted for each time point. Data represent mean ± SD of three independent experiments. The difference in foci number between ATM+ and ATM− cells 10 or 20 min after irradiation was significant at $P < 0.001$ using a Student's t test. (C) Wortmannin inhibits γ-radiation–induced 53BP1 foci formation. HeLa cells were pretreated for 30 min with 0, 50, or 200 μM wortmannin before exposure to 1 Gy of γ-radiation. After recovery for 1 h, the control or irradiated cells were immunostained with anti-53BP1 antibodies.

readily detected in cells that had received no drug treatment before radiation. We next repeated the experiment using the ATM-deficient GM03189D and GM02184D cells expressing wild-type ATM. Again, in ATM wild-type cells, γ-radiation induced a 53BP1 mobility shift in control, but not in wortmannin-pretreated samples (Fig. 4 C). However, no radiation-induced 53BP1 mobility shift was observed in ATM-deficient cells, with or without wortmannin treatment (Fig. 4, C and D). Taken together, these results strongly suggest that ATM is required for 53BP1 hyperphosphorylation after γ-radiation.

53BP1 Is a Substrate of ATM In Vitro

S/TQ sites have been described to be the minimal essential recognition sites for ATM (Kim et al., 1999). 53BP1 contains a total of 30 S/TQ sites, many of them clustered in the

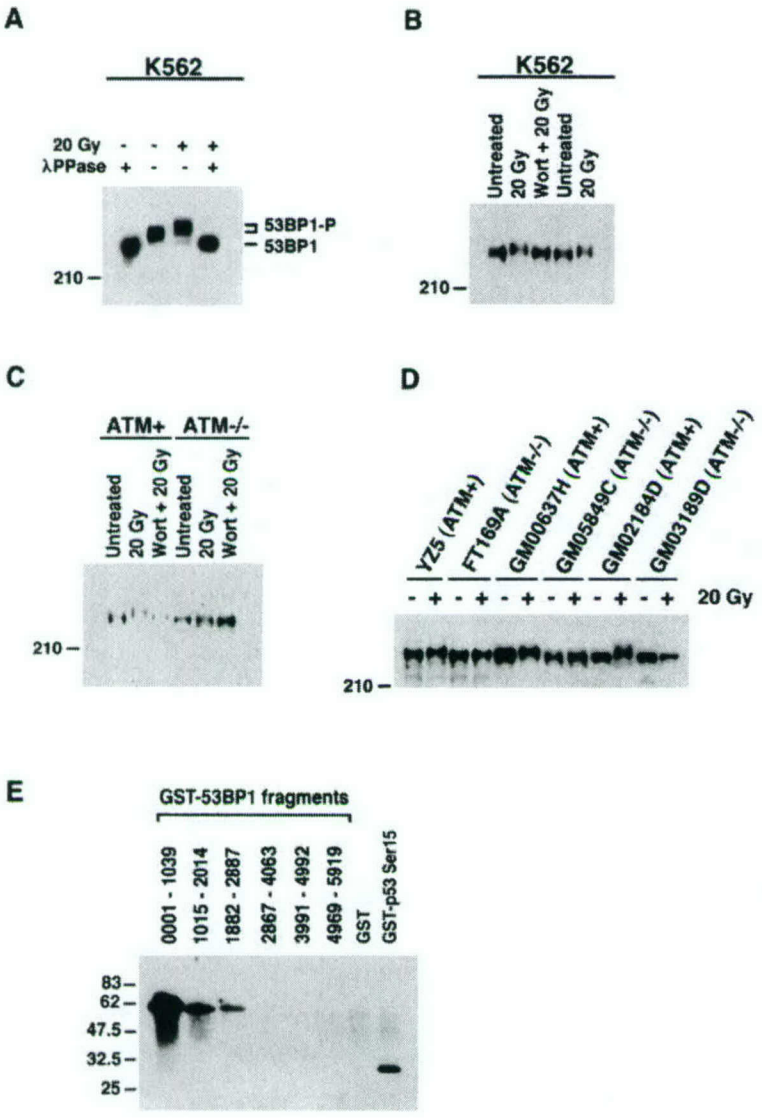

Figure 4. γ-Radiation–induced hyperphosphorylation of 53BP1 requires ATM. (A) γ-Radiation induces hyperphosphorylation of 53BP1. K562 cells were exposed to 0 or 20 Gy of γ-radiation and immunoprecipitated using polyclonal anti-53BP1 antibody. Immunoprecipitates were incubated for 1 h at 30°C with 800U λ-phosphatase (λPPase) in 100 μl incubation buffer or only incubation buffer. The samples were separated on a 3–8% gel and immunoblotted with anti-53BP1. (B) Wortmannin inhibits 53BP1 hyperphosphorylation. K562 cells were pretreated with 50 μM wortmannin for 30 min before exposure to 1 Gy of radiation. Whole cell lysates prepared from treated and control samples were separated on a 3–8% gradient gel (30 μg protein per lane) and immunoblotted with anti-53BP1 antibodies. (C) ATM is required for the γ-radiation–induced hyperphosphorylation of 53BP1. ATM-deficient GM03189D cells or ATM wild-type GM02184D cells were treated as described in the legend to B, and 30 μg lysates were separated on a 3–8% gel before immunoblotting with anti-53BP1 antibodies. (D) All three ATM-deficient cell lines tested (FT169A, GM03189D, and GM05849C) show no hyperphosphorylation 1 h after 20 Gy. (E) 53BP1 is a substrate of ATM in vitro. Six GST fusion proteins containing overlapping 53BP1 fragments were used as substrates in an ATM in vitro kinase assay. GST protein alone and GST fusion protein containing 13 residues surrounding the serine-15 of the p53 coding sequence were used, respectively, as negative and positive controls.

NH_2-terminal region. To examine whether 53BP1 is a substrate for ATM, and to define regions that can be phosphorylated by ATM in vitro, we designed six overlapping 53BP1 GST fragments that span the entire ORF of 53BP1 and performed a standard ATM kinase assay. As shown in Fig. 4 E, the first three NH_2-terminal 53BP1 fragments were phosphorylated by ATM in vitro, whereas no phosphorylation was observed in the last three COOH-terminal fragments, despite the fact that there are a total of 10 S/TQ sites within these 53BP1 fragments. These data suggest that 53BP1 is a substrate of ATM kinase.

Discussion

Here we report that 53BP1 participates in the early DNA damage–response. Using several antibodies specifically recognizing 53BP1, we show that 53BP1 becomes hyperphosphorylated and forms nuclear foci after exposure to ionizing radiation. γ-Radiation–induced 53BP1 hyperphosphorylation and foci formation are reduced in ATM-deficient cells. Moreover, 53BP1 hyperphosphorylation, as well as foci formation, is inhibited by wortmannin, an inhibitor of the PI3K-related kinases including ATM, DNA-PK, and, to a lesser extent, ATR (Sarkaria et al., 1998). Taken together, these data suggest that ATM and other PI3K-related kinases directly phosphorylate 53BP1 and regulate its localization to the sites of DNA strand breaks.

In favor of a functional link between ATM and 53BP1, we also demonstrate that NH_2-terminal fragments of 53BP1 are effectively phosphorylated by ATM in vitro. Similarly, Xia and colleagues have recently shown that *Xenopus* 53BP1 and a NH_2-terminal fragment of human 53BP1 can be phosphorylated by ATM in vitro and in vivo (Xia et al., 2000), supporting our hypothesis that 53BP1 is a direct substrate of ATM. In contrast to our findings, Schultz et al. (2000) observed no difference in 53BP1 foci formation in ATM-deficient cells when compared with that in normal ATM wild-type cells (Schultz et al., 2000). We also observed that 53BP1 foci still formed, albeit with slower kinetics, in cells lacking ATM, suggesting the exist-

ence of an alternative, ATM-independent pathway for the regulation of 53BP1. However, our data presented here clearly demonstrate that ATM plays a critical role in the regulation of 53BP1 hyperphosphorylation and foci formation after γ-radiation.

53BP1 rapidly colocalizes with γ-H2AX in response to ionizing radiation. H2AX is a histone H2A variant that becomes phosphorylated and forms foci at sites of DNA strand breaks after DNA damage (Rogakou et al., 1999; Paull et al., 2000). The number, as well as appearance and disappearance of 53BP1 foci, matched almost completely with that of γ-H2AX. Moreover, 53BP1 and γ-H2AX physically interact after ionizing radiation, suggesting that 53BP1 relocates to the sites of DNA double strand breaks in response to γ-radiation. Similar to 53BP1, γ-H2AX foci formation is inhibited by wortmannin treatment (Rogakou et al., 1999; Paull et al., 2000) and is reduced in ATM-deficient cells (Rappold, I., and J. Chen, unpublished observation). It is possible that phosphorylation of H2AX may mediate the relocalization of 53BP1 to DNA strand breaks. If this is the case, ATM-dependent hyperphosphorylation of 53BP1 may be a secondary event that is not required for 53BP1 foci formation. This possibility will be examined in future studies using phosphorylation-deficient mutants of 53BP1.

Upon relocalizing to the sites of DNA damage, 53BP1 could participate in chromosome remodeling that makes DNA lesions accessible to DNA repair proteins. Alternatively, 53BP1 could be involved in the recruitment of repair proteins like BRCA1 and Rad51 to these DNA lesions. Both of these proteins colocalize with 53BP1 several hours after exposure to ionizing radiation (Rappold, I., and J. Chen, unpublished observations). In addition, BRCA1 biochemically interacts with 53BP1 after γ-radiation (Rappold, I., and J. Chen, unpublished observations).

53BP1 contains two BRCT motifs at its COOH terminus. 53BP1 BRCT motifs are closely related with those of BRCA1 and *Saccharomyces cerevisiae* Rad9 (scRad9) protein. Insight into the potential role of scRad9 comes from studies of its association with scRad53. ScRad53 is the homologue of mammalian Chk2 or *Schizosaccharomyces pombe* Cds1. After DNA damage, scRad9 is phosphorylated and this phosphorylated scRad9 associates with the forkhead homology–associated (FHA) domain of scRad53 (Sun et al., 1998; Vialard et al., 1998). Mutations in either the scRad53 FHA domain (Sun et al., 1998) or scRad9 BRCT motifs (Soulier and Lowndes, 1999) prevent scRad53 activation after DNA damage. Although the mammalian homologue of scRad9 has not been identified, a scRad9 homologue likely exists in mammals. Because of the close homology of their BRCT motifs, two candidate scRad9 homologues are BRCA1 and 53BP1. Based on yeast studies, one would predict that the activation of Chk2, the homologue of scRad53, should depend on this scRad9 homologue in mammalian cells. However, DNA damage–induced phosphorylation of Chk2 was observed in BRCA1-deficient cells (Matsuoka et al., 1998), suggesting that BRCA1 may not be the mammalian homologue of scRad9. Experiments using 53BP1-deficient cells will be performed to examine whether 53BP1 is the scRad9 homologue in mammals.

In conclusion, our data demonstrate that 53BP1 participates early in DNA damage–signaling pathways and is regulated by ATM after γ-radiation. The exact role of 53BP1 in these pathways remains to be resolved. Given the importance of these DNA damage–signaling pathways in cancer prevention, it will be interesting to examine whether 53BP1 is mutated in tumors.

We thank Drs. Scott Kaufmann, Larry Karnitz, and Jann Sarkaria for stimulating conversations. We also thank the Mayo Clinic Flow Cytometry and Protein Core facilities for their assistance. Initial studies of this work were performed in the laboratory of Dr. David M. Livingston. We specially thank Dr. Livingston for help and encouragement during the course of this study.

This work was supported by the Mayo Foundation, Mayo Cancer Center, Division of Oncology Research, and an Eagles grant to J. Chen.

Submitted: 24 October 2000
Revised: 23 March 2001
Accepted: 26 March 2001

References

Appella, E., and C.W. Anderson. 2000. Signaling to p53: breaking the post-translational modification code. *Pathol. Biol. (Paris)*. 48:227–245.

Bork, P., K. Hofmann, P. Bucher, A.F. Neuwald, S.F. Altschul, and E.V. Koonin. 1997. A superfamily of conserved domains in DNA damage-responsive cell cycle checkpoint proteins. *FASEB J.* 11:68–76.

Callebaut, I., and J.P. Mornon. 1997. From BRCA1 to RAP1: a widespread BRCT module closely associated with DNA repair. *FEBS Lett.* 400:25–30.

Canman, C.E., D.S. Lim, K.A. Cimprich, Y. Taya, K. Tamai, K. Sakaguchi, E. Appella, M.B. Kastan, and J.D. Siliciano. 1998. Activation of the ATM kinase by ionizing radiation and phosphorylation of p53. *Science*. 281:1677–1679.

Chai, Y.L., J. Cui, N. Shao, E. Shyam, P. Reddy, and V.N. Rao. 1999. The second BRCT domain of BRCA1 proteins interacts with p53 and stimulates transcription from the p21WAF1/CIP1 promoter. *Oncogene*. 18:263–268.

Iwabuchi, K., P.L. Bartel, B. Li, R. Marraccino, and S. Fields. 1994. Two cellular proteins that bind to wild-type but not mutant p53. *Proc. Natl. Acad. Sci. USA*. 91:6098–6102.

Iwabuchi, K., B. Li, H.F. Massa, B.J. Trask, T. Date, and S. Fields. 1998. Stimulation of p53-mediated transcriptional activation by the p53-binding proteins, 53BP1 and 53BP2. *J. Biol. Chem*. 273:26061–26068.

Khanna, K.K. 2000. Cancer risk and the ATM gene: a continuing debate. *J. Natl. Cancer Inst*. 92:795–802.

Khanna, K.K., K.E. Keating, S. Kozlov, S. Scott, M. Gatei, K. Hobson, Y. Taya, B. Gabrielli, D. Chan, S.P. Lees-Miller, and M.F. Lavin. 1998. ATM associates with and phosphorylates p53: mapping the region of interaction. *Nat. Genet*. 20:398–400.

Kim, S.T., D.S. Lim, C.E. Canman, and M.B. Kastan. 1999. Substrate specificities and identification of putative substrates of ATM kinase family members. *J. Biol. Chem*. 274:37538–37543.

Koonin, E.V., S.F. Altschul, and P. Bork. 1996. BRCA1 protein products...Functional motifs... *Nat. Genet*. 13:266–268.

Lees-Miller, S.P., R. Godbout, D.W. Chan, M. Weinfeld, R.S. Day, 3rd, G.M. Barron, and J. Allalunis-Turner. 1995. Absence of p350 subunit of DNA-activated protein kinase from a radiosensitive human cell line. *Science*. 267: 1183–1185.

Matsuoka, S., M. Huang, and S.J. Elledge. 1998. Linkage of ATM to cell cycle regulation by the Chk2 protein kinase. *Science*. 282:1893–1897.

Ouchi, T., A.N. Monteiro, A. August, S.A. Aaronson, and H. Hanafusa. 1998. BRCA1 regulates p53-dependent gene expression. *Proc. Natl. Acad. Sci. USA*. 95:2302–2306.

Paull, T.T., E.P. Rogakou, V. Yamazaki, C.U. Kirchgessner, M. Gellert, and W.M. Bonner. 2000. A critical role for histone H2AX in recruitment of repair factors to nuclear foci after DNA damage. *Curr. Biol*. 10:886–895.

Rogakou, E.P., C. Boon, C. Redon, and W.M. Bonner. 1999. Megabase chromatin domains involved in DNA double-strand breaks in vivo. *J. Cell Biol*. 146:905–916.

Sarkaria, J.N., R.S. Tibbetts, E.C. Busby, A.P. Kennedy, D.E. Hill, and R.T. Abraham. 1998. Inhibition of phosphoinositide 3-kinase related kinases by the radiosensitizing agent wortmannin. *Cancer Res*. 58:4375–4382.

Schultz, L.B., N.H. Chehab, A. Malikzay, and T.D. Halazonetis. 2000. p53 binding protein 1 (53BP1) is an early participant in the cellular response to DNA double-strand breaks. *J. Cell Biol*. 151:1381–1390.

Scully, R., J. Chen, A. Plug, Y. Xiao, D. Weaver, J. Feunteun, T. Ashley, and D.M. Livingston. 1997. Association of BRCA1 with Rad51 in mitotic and meiotic cells. *Cell*. 88:265–275.

Smith, G.C., and S.P. Jackson. 1999. The DNA-dependent protein kinase.

Genes Dev. 13:916–934.

Soulier, J., and N.F. Lowndes. 1999. The BRCT domain of the *S. cerevisiae* checkpoint protein Rad9 mediates a Rad9-Rad9 interaction after DNA damage. *Curr. Biol.* 9:551–554.

Sun, Z., J. Hsiao, D.S. Fay, and D.F. Stern. 1998. Rad53 FHA domain associated with phosphorylated Rad9 in the DNA damage checkpoint. *Science.* 281:272–274.

Vialard, J.E., C.S. Gilbert, C.M. Green, and N.F. Lowndes. 1998. The budding yeast Rad9 checkpoint protein is subjected to Mec1/Tel1-dependent hyperphosphorylation and interacts with Rad53 after DNA damage. *EMBO (Eur. Mol. Biol. Organ.) J.* 17:5679–5688.

Xia, Z., J.C. Morales, W.G. Dunphy, and P.B. Carpenter. 2000. Negative cell cycle regulation and DNA-damage inducible phosphorylation of the BRCT protein 53BP1. *J. Biol. Chem.* 276:2708–2718.

Zhang, H., K. Somasundaram, Y. Peng, H. Tian, D. Bi, B.L. Weber, and W.S. El-Deiry. 1998a. BRCA1 physically associates with p53 and stimulates its transcriptional activity. *Oncogene.* 16:1713–1721.

Zhang, X., S. Morera, P.A. Bates, P.C. Whitehead, A.I. Coffer, K. Hainbucher, R.A. Nash, M.J. Sternberg, T. Lindahl, and P.S. Freemont. 1998b. Structure of an XRCC1 BRCT domain: a new protein-protein interaction module. *EMBO (Eur. Mol. Biol. Organ.) J.* 17:6404–6411.

Ziv, Y., A. Bar-Shira, I. Pecker, P. Russell, T.J. Jorgensen, I. Tsarfati, and Y. Shiloh. 1997. Recombinant ATM protein complements the cellular A-T phenotype. *Oncogene.* 15:159–167.

Accelerated Publication

THE JOURNAL OF BIOLOGICAL CHEMISTRY
Vol. 278, No. 22, Issue of May 30, pp. 19579–19582, 2003

Accumulation of Checkpoint Protein 53BP1 at DNA Breaks Involves Its Binding to Phosphorylated Histone H2AX*

Received for publication, March 14, 2003,
and in revised form, April 15, 2003
Published, JBC Papers in Press, April 15, 2003,
DOI 10.1074/jbc.C300117200

Irene M. Ward‡§, Kay Minn‡, Katherine G. Jorda¶, and Junjie Chen‡‖

From the ‡Department of Oncology, Mayo Clinic and Foundation, Rochester, Minnesota 55905 and the ¶Division of Oncology, Columbia University, New York, New York 10032

53BP1 participates in the cellular response to DNA damage. Like many proteins involved in the DNA damage response, 53BP1 becomes hyperphosphorylated after radiation and colocalizes with phosphorylated H2AX in megabase regions surrounding the sites of DNA strand breaks. However, it is not yet clear whether the phosphorylation status of 53BP1 determines its localization or vice versa. In this study we mapped a region upstream of the 53BP1 C terminus that is required and sufficient for the recruitment of 53BP1 to these DNA break areas. *In vitro* assays revealed that this region binds to phosphorylated but not unphosphorylated H2AX. Moreover, using H2AX-deficient cells reconstituted with wild-type or a phosphorylation-deficient mutant of H2AX, we have shown that phosphorylation of H2AX at serine 140 is critical for efficient 53BP1 foci formation, implying that a direct interaction between 53BP1 and phosphorylated H2AX is required for the accumulation of 53BP1 at DNA break sites. On the other hand, radiation-induced phosphorylation of the 53BP1 N terminus by the ATM (ataxia-telangiectasia mutated) kinase is not essential for 53BP1 foci formation and takes place independently of 53BP1 redistribution. Thus, these two damage-induced events, hyperphosphorylation and relocalization of 53BP1, occur independently in the cell.

The DNA of eukaryotic cells is constantly exposed to endogenous and exogenous DNA-damaging agents. To prevent the accumulation of genomic damage and avert cellular dysfunction, cells have evolved complex response mechanisms. 53BP1 was initially identified as a protein that binds to the central DNA binding domain of p53 and enhances p53-mediated transcriptional activation (1, 2). In response to genotoxic stress, 53BP1 rapidly redistributes from a diffuse nuclear localization into distinct nuclear foci suggesting that 53BP1 is involved in the DNA damage response (3–6). Moreover the C terminus of 53BP1 contains two BRCT domains, a motif found in a number of proteins implicated in various aspects of cell cycle control, recombination, and DNA repair (7, 8). Subsequent studies have shown that 53BP1 becomes hyperphosphorylated in response to ionizing radiation (IR)[1] and colocalizes with phosphorylated histone H2AX (γ-H2AX) at the sites of DNA lesions (3, 4). Other proteins known to be involved in the DNA damage signaling pathway (*i.e.* BRCA1, Rad51, NBS1, and TopoBP1) were also found to colocalize with 53BP1 in these inducible foci (3, 4, 6, 9). Direct evidence for an important role of 53BP1 in the DNA damage response came recently from studies using 53BP1-deficient cells. Human cell lines treated with specific small interfering RNA to silence 53BP1 expression exhibited a defect in the intra-S phase checkpoint and, at low IR doses, a partial defect in the G_2-M checkpoint (10–12). Moreover 53BP1-deficient mice are hypersensitive to ionizing radiation and show an increased incidence of developing thymic lymphomas (13). Several lines of evidence suggest that 53BP1 is a substrate of ATM, the kinase mutated in the human disease ataxia-telangiectasia, and is involved in the phosphorylation of various ATM substrates (3, 6, 10).

Despite this recent progress made toward 53BP1 function little is known about the initial activation of 53BP1. Recruitment of 53BP1 to γ-H2AX foci seems to be a crucial step. H2AX-deficient cells lack normal 53BP1 foci formation and, like 53BP1-deficent cells, manifest a G_2-M checkpoint defect after exposure to low doses of ionizing radiation (12). Moreover, H2AX−/− mice show a radiation sensitivity similar to 53BP1−/− mice (14). In this study we mapped the region required for 53BP1 foci formation in response to DNA damage. We show that a region upstream of the BRCT motifs is sufficient for 53BP1 foci formation and that this region interacts directly with phosphorylated H2AX. Using H2AX-deficient cells retransfected with either wild-type H2AX or an H2AX phosphomutant we confirm that phosphorylation of H2AX at Ser-140 is required for 53BP1 accumulation at DNA break areas. In contrast, radiation-induced phosphorylation of 53BP1 by ATM is not essential for the recruitment of 53BP1 to foci and occurs independently.

EXPERIMENTAL PROCEDURES

Plasmid Constructs and Transfection—53BP1 deletion mutants were generated by inserting stop codons and/or restriction sites at various positions into pCMH6K 53BP1 (2) using the QuikChange site-directed mutagenesis kit (Stratagene). A 3×NLS (nuclear localization sequence) was inserted into the *Nhe*I site upstream of the N-terminal hemagglutinin (HA) and His_6 tags. U2OS cells were transfected using FuGENE 6 (Roche Applied Science) according to the manufacturer's instructions. H2AX was PCR-amplified from human genomic DNA and inserted between the HA tag and an internal ribosomal entry site fused to the puromycin gene of a modified pcDNA3 vector. The H2AX phosphomutant was generated by replacing Ser-140 of H2AX with an alanine using the QuikChange mutagenesis kit (Stratagene). H2AX-deficient embry-

* This work was supported by grants from the National Institutes of Health, Breast Cancer Research Foundation, and Prospect Creek Foundation. The costs of publication of this article were defrayed in part by the payment of page charges. This article must therefore be hereby marked "*advertisement*" in accordance with 18 U.S.C. Section 1734 solely to indicate this fact.

§ Supported by a postdoctoral fellowship from the Department of Defense breast cancer research program.

‖ Recipient of a Department of Defense breast cancer career development award. To whom correspondence should be addressed. Tel.: 507-538-1545; Fax: 507-284-3906; E-mail: Chen.junjie@mayo.edu.

[1] The abbreviations used are: IR, ionizing radiation; γ-H2AX, phosphorylated histone H2AX; ATM, ataxia-telangiectasia mutated; NLS, nuclear localization sequence; HA, hemagglutinin; ES, embryonic stem; KLH, keyhole limpet hemocyanin; Gy, gray(s); GST, glutathione *S*-transferase; aa, amino acid(s); IF, immunofluorescence; BRCT, BRCA1 C terminus.

onic stem (ES) cells (provided by C. Bassing, Ref. 15) were transfected by electroporation.

Antibodies—Anti-S6P, anti-S25P/29P, and anti-S784P specific antibodies were generated by coupling synthetic 53BP1 peptides (S6P, CDPTG(P)SQLD; S25P/29P, CIED(P)SQPE(P)SQVLEDD; S784P, CSD(P)SQSWEDI where (P)S represents phosphoserine) to KLH using Imject maleimide-activated mcKLH (Pierce) prior to immunizing rabbits (Cocalico Biological). The antibodies were affinity-purified on agarose columns coupled with the non-phosphorylated or phosphorylated peptide (SulfoLink Coupling Gel, Pierce). Anti-53BP1 and anti-γ-H2AX antibodies were generated as described previously (3). Monoclonal antibody HA11 specific for HA was purchased from BabCO Berkeley Antibody Co. Anti-ATM antibody Ab3 was purchased from Oncogene Research Products.

Immunofluorescence Staining, Immunoblots, and Immunoprecipitation—Cells grown on coverslips were fixed with 3% paraformaldehyde 1 h after exposure to 0 or 1 Gy of IR. After permeabilization with 0.5% Triton X-100, cells were blocked with 5% goat serum and incubated successively with the primary and secondary antibodies, each for 25 min at 37 °C. In case of DNase or RNase treatment, cells were irradiated, permeabilized with 0.5% Triton X-100 for 3 min, and incubated with either DNase I (10 units/ml) or RNase A (50 μg/ml) in phosphate-buffered saline plus calcium and magnesium for 30 min at 37 °C prior to fixation with 3% paraformaldehyde. Immunoprecipitation and immunoblot assays were done as described previously (3).

ATM Kinase Assays—ATM was precipitated from K562 cells, and aliquots of the ATM-protein A-Sepharose immunocomplex were resuspended in 25 μl of kinase buffer (10 mM Hepes (pH 7.4), 50 mM NaCl, 10 mM $MgCl_2$, 10 mM $MnCl_2$, 1 mM dithiothreitol, 10 nM ATP). ATM kinase reactions were carried out at 30 °C for 20 min with 10 μCi of [γ-^{32}P]ATP and 1 μg of 53BP1 GST fusion proteins.

GST Pull-down Assays—GST pull-down experiments were performed by incubating 3 μg of various GST-labeled 53BP1 fragments with C-terminal H2AX peptide that was either phosphorylated or unphosphorylated at Ser-140 (CKATQA(P)SQEY) and had been immobilized on SulfoLink Coupling Gel (Pierce). Bound GST proteins were isolated by incubating the mixture for 1 h at 4 °C in 200 μl of NETN buffer (150 mM NaCl, 1 mM EDTA, 20 mM Tris (pH 8), 0.5% Nonidet P-40), washing five times with NETN, eluting the proteins with 2× Laemmli buffer, separating them by SDS-PAGE, and immunoblotting with horseradish peroxidase-conjugated anti-GST (B-14, Santa Cruz Biotechnology).

Generation of 53BP1-deficient Embryonic Cells—A 53BP1-deficient embryonic cell line was derived from 53BP1−/− blastocysts using a standard procedure. The generation of 53BP1-deficient mice is described in Ref. 13.

RESULTS

A Region Upstream of the Tandem BRCT Motif Is Required and Sufficient for 53BP1 Foci Formation—53BP1 is a large 1972-aa nuclear protein with a C-terminal tandem BRCT motif. Upstream of the BRCT repeats resides a bipartite nuclear localization signal (predictNLS, Ref. 16) and a tudor domain (RPS-BLAST, Ref. 17), a motif found in several RNA-binding proteins. In response to IR, 53BP1 rapidly redistributes to distinct nuclear foci that colocalize with γ-H2AX (3, 4, 6). Treatment of irradiated cells with DNase, but not RNase, completely abolished 53BP1 and γ-H2AX foci formation confirming that these foci localize to DNA (Fig. 1*A*).

To determine the minimal region required for the recruitment of 53BP1 to damage-induced foci, we generated various HA-tagged 53BP1 deletion mutants and examined their distribution in transiently transfected U2OS cells (Fig. 1, *B* and *C*, and data not shown). A 3×NLS motif fused to the N terminus of 53BP1 ensured nuclear expression of the various constructs. Truncation of the 53BP1 N terminus (Δ1–1052) or the BRCT domains (Δ1700–1972) did not affect 53BP1 foci formation as assessed by IF 1 h after exposure to 1 Gy of IR (Fig. 1*C*). However, increasing C-terminal deletions (Δ1305–1972 and Δ1052–1972) or deletion of a region upstream of the tandem BRCT motifs (Δ1052–1305) abolished 53BP1 foci formation (Fig. 2, *B* and *C*, and data not shown). Moreover a 53BP1 construct expressing residues 1052–1639 including the tudor domain was found to be sufficient for 53BP1 foci formation (Fig. 1, *B* and *C*) suggesting that the domain required for foci formation is contained within this region.

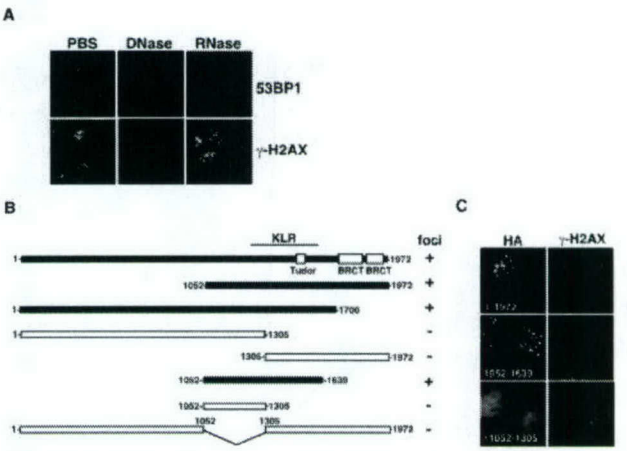

FIG. 1. **A region upstream of the BRCT domains is required and sufficient for damage-induced focus localization of 53BP1.** *A*, DNase but not RNase treatment abolishes 53BP1 and γ-H2AX foci formation in response to 1 Gy of IR. *B*, schematic diagram of the wild-type or mutant 53BP1 constructs that were N-terminally fused to a 3×NLS and an HA tag. Their abilities to form damage-induced foci is indicated by a +. *KLR* refers to the kinetochore localization region. *C*, U20S cells transiently expressing the HA-53BP1 constructs were irradiated with 1 Gy and immunostained 1 h later with anti-HA and anti-γ-H2AX antibodies. *PBS*, phosphate-buffered saline.

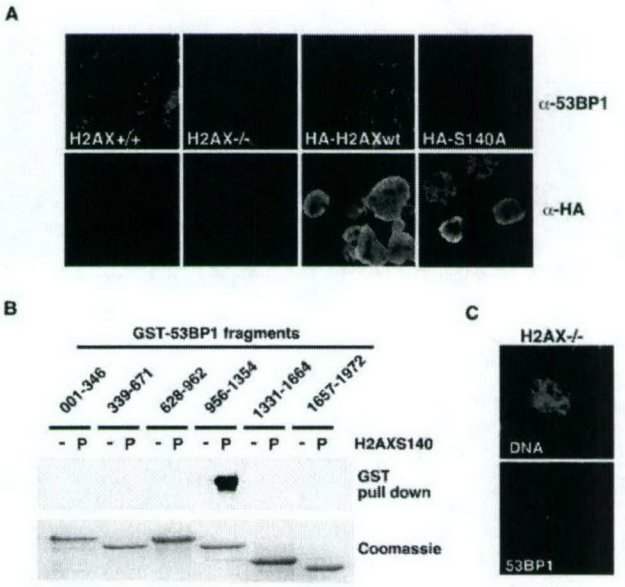

FIG. 2. **53BP1 foci formation requires its binding to phosphorylated Ser-140 of H2AX.** *A*, H2AX−/− ES cells were transiently transfected with either HA-tagged wild-type H2AX (*HA-H2AXwt*) or a S140A phosphorylation-deficient mutant (*HA-S140A*). 53BP1 foci formation was assessed by IF 1 h after exposure of cells to 1 Gy of IR. *B*, GST-53BP1 fragments, encoding different regions of 53BP1 as indicated, were incubated with immobilized C-terminal H2AX peptide that was either phosphorylated (*P*) or not at Ser-140. Pulled down proteins were separated by SDS-PAGE followed by immunoblotting with anti-GST antibodies. The addition of similar amounts of various GST proteins was verified by SDS-PAGE and Coomassie Blue staining. *C*, H2AX−/− cells were stained with anti-53BP1 antibodies and 4,6-diamidino-2-phenylindole, and mitotic cells were analyzed for kinetochore localization of 53BP1.

53BP1 Focus Localization Region Interacts Directly with γ-H2AX—H2AX-deficient cells show greatly reduced 53BP1 foci formation implying that H2AX is involved in the recruit-

ment of 53BP1 to radiation-induced foci (14). H2AX becomes phosphorylated at a conserved C-terminal SQ site upon exposure of cells to ionizing radiation (18). Phosphorylation of H2AX at Ser-140 is impaired in ATM-deficient cells suggesting that this site is dominantly phosphorylated by ATM (12). To analyze whether phosphorylation of H2AX at Ser-140 is required for 53BP1 redistribution we transiently expressed wild-type H2AX or a S140A phosphomutant in H2AX-deficient ES cells and assessed 53BP1 foci formation. As shown in Fig. 2*A*, expression of wild-type H2AX reconstituted 53BP1 foci formation in response to IR. In marked contrast, expression of the H2AX S140A phosphomutant was insufficient to induce 53BP1 accumulation at the sites of DNA strand breaks.

We had shown earlier that phosphorylated H2AX co-immunoprecipitates with 53BP1 upon exposure of cells to DNA damage (3). To determine whether the region required for 53BP1 focus localization interacts directly with γ-H2AX, we used an *in vitro* pull-down assay. Six different 53BP1 GST fragments spanning the entire 53BP1 protein were incubated with immobilized C-terminal H2AX peptide that was either phosphorylated or non-phosphorylated at Ser-140. Only 53BP1 fragment 956–1354, which overlaps with the mapped focus localization region, showed strong interaction with the phosphorylated H2AX peptide (Fig. 2*B*). As a control, no binding was detected to the non-phosphorylated peptide bearing identical sequence (Fig. 2*B*).

Since H2AX directs 53BP1 accumulation in response to DNA damage, we asked whether H2AX is also required for the kinetochore localization of 53BP1 in mitotic cells (19). As shown in Fig. 2*C*, 53BP1 can be readily detected at the kinetochores in H2AX-deficient mitotic cells suggesting that the kinetochore localization of 53BP1 is not mediated by phospho-H2AX.

Phosphorylation of 53BP1 Is Not Required for Foci Formation—We had previously demonstrated that 53BP1 becomes hyperphosphorylated in response to IR, and three regions at the N terminus of 53BP1 were found to be phosphorylated by ATM *in vitro* (3). To map the phosphorylation sites we designed a series of GST fusion peptides containing one or two ATM binding motifs (SQ or TQ sites). ATM kinase assays using these purified GST fusion proteins as substrates, and ATM kinase immunoprecipitated from either K562 lysates (containing wild-type ATM) or ATM-deficient GM03189D lysates revealed peptides aa 1–12, aa 18–37, and aa 778–791 as putative ATM substrates (Fig. 3*A*). To examine whether the respective SQ sites become phosphorylated *in vivo*, we raised polyclonal antibodies against phosphorylated Ser-6 (anti-S6P), phosphorylated Ser-25 and Ser-29 (anti-S25P/29P), and phosphorylated Ser-784 (anti-S784P). All affinity-purified antisera recognized 53BP1 in irradiated cells but not in untreated controls when assessed by immunofluorescence analysis (data not shown). In addition, anti-53BP1 S25P/29P antibodies detected 53BP1 from irradiated ATM wild-type but not ATM-deficient cells by Western blot analyses (Fig. 3*B*). Pretreatment with λ-phosphatase abolished the antibody binding further validating that anti-53BP1 S25P/29P specifically recognizes the phosphorylated form of 53BP1 (Fig. 3*B*).

To test whether phosphorylation of 53BP1 is required for the recruitment of 53BP1 to sites of DNA lesions, we generated a phosphorylation-deficient mutant (53BP1 4SA) by mutating the mapped ATM target sites (Ser-6, Ser-25/Ser-29, and Ser-784) to alanines. 53BP1−/− embryonic cells transfected with this phosphomutant showed normal 53BP1 foci formation in response to IR (Fig. 3*C*), indicating that ATM-dependent phosphorylation of 53BP1 is not required for recruitment to or retention of 53BP1 at DNA break sites.

Phosphorylation of 53BP1 might occur at the break areas. To test this possibility, we transiently transfected 53BP1-deficient embryonic cells with the HA-tagged mutant that lacks part of the 53BP1 focus localization region (Δ1052–1305) and remains a diffuse nuclear localization upon exposure of cells to IR. Co-immunostaining with anti-HA and anti-53BP1 S25P/29P antibodies revealed that ATM-dependent 53BP1 phosphorylation does not require 53BP1 foci formation (Fig. 3*D*). Immunoprecipitation assays confirmed that 53BP1 Δ1052–1305 becomes readily phosphorylated at Ser-25/Ser-29 in response to IR (Fig. 3*E*). These findings are consistent with a recent report describing phosphorylation of 53BP1 Ser-25 in H2AX-deficient cells (12). Taken together, these results suggest that 53BP1 focus localization and ATM-dependent phosphorylation of 53BP1 are regulated independently.

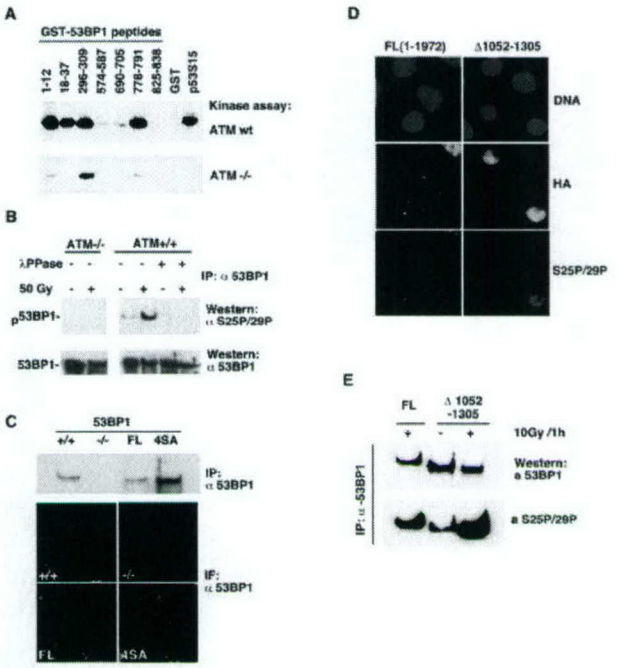

FIG. 3. **Damage-induced phosphorylation of 53BP1 occurs independently of 53BP1 foci formation.** *A*, *in vitro* mapping of potential ATM phosphorylation sites. ATM kinase assays were performed using ATM kinase immunoprecipitated from K562 lysates (ATM wild type) or GM03189D lysates (ATM-deficient) and GST fusion peptides containing one or two SQ or TQ sites of 53BP1. GST or GST fusion protein containing 14 amino acids surrounding the Ser-15 of p53 (*p53S15*) were used as negative and positive controls, respectively. *B*, 53BP1 is phosphorylated *in vivo* following IR. 293T cells containing wild-type ATM and ATM-deficient GM03189D cells were mock-treated or irradiated (50 Gy). After 1 h, whole cell lysates were immunoprecipitated with anti-53BP1 antibody. Duplicate samples were treated with or without λ-phosphatase (*λPPase*). Western blots were performed with anti-53BP1 or an anti-phospho-53BP1 antiserum raised against the phosphoserines 25/29 of 53BP1. *C*, ATM-dependent 53BP1 phosphorylation is not required for 53BP1 foci formation. HA-tagged full-length 53BP1 (*FL*) or a phosphorylation-deficient mutant of 53BP1 (*4SA*) were stably expressed in 53BP1-deficient embryonic cells. 53BP1 expression levels were assessed by immunoprecipitation. 53BP1 foci formation was analyzed by IF 1 h after 1 Gy of IR. *D*, 53BP1 foci formation is not required for ATM-dependent phosphorylation of 53BP1 following DNA damage. 53BP1-deficient embryonic cells were transiently transfected with HA-tagged full-length 53BP1 or a deletion mutant lacking part of the focus formation region. 53BP1 localization and ATM-dependent phosphorylation was analyzed 1 h after 1 Gy of IR by co-staining with anti-HA antibody and anti-phospho-53BP1 antiserum (anti-25P/29P). *E*, an aliquot of the transfected cells was either mock-treated or irradiated with 10 Gy. 53BP1 was immunoprecipitated from cell lysates, and phosphorylation of 53BP1 was analyzed by immunoblotting with the 53BP1 phosphospecific anti-S25P/29P antibodies. *wt*, wild type; *IP*, immunoprecipitation.

DISCUSSION

Upon exposure of cells to genotoxic stress, 53BP1 rapidly redistributes from a pan-nuclear localization to distinct nuclear foci at the sites of DNA strand breaks. In this study we have mapped the region required for 53BP1 foci formation and examined the role of H2AX in 53BP1 accumulation. Moreover, we provided evidence that phosphorylation of 53BP1 by the ATM kinase occurs independently of 53BP1 foci formation.

53BP1 had been speculated to be involved in the DNA damage response based on its C-terminal tandem BRCT domains. This motif was first detected in the BRCA1 C terminus and has been reported to bind directly to DNA breaks (20). Surprisingly the BRCT domains of 53BP1 were found to be dispensable for 53BP1 foci formation. Instead a region upstream of the BRCT motifs proved to be essential for 53BP1 accumulation at sites of DNA strand breaks. Our data suggest that the damage-induced phosphorylation of H2AX directs 53BP1 accumulation at sites of DNA strand breaks. First, H2AX-deficient cells reconstituted with a H2AX phosphomutant failed to induce or sustain 53BP1 foci formation. Second, a 53BP1 fragment (residues 956–1354) contained within the 53BP1 focus localization region interacted strongly with phosphorylated H2AX *in vitro*. Third, 53BP1 co-immunoprecipitates with H2AX in a DNA damage-dependent manner (3). Thus, it is likely that the DNA damage-induced phosphorylation of H2AX at Ser-140 increases the interaction between H2AX and 53BP1 and leads to the accumulation of 53BP1 at the sites of DNA breaks.

Interestingly the focus localization region we mapped includes a region required for 53BP1 kinetochore localization in mitotic cells (residues 1220–1601) (19). Very recently, Morales and colleagues (21) showed that the kinetochore localization region is also essential for 53BP1 foci formation in response to DNA damage suggesting that both events might be regulated in a similar fashion. However, the kinetochore localization of 53BP1 is unlikely to involve DNA lesions (19). We have shown that 53BP1 kinetochore localization appears normal in H2AX-deficient cells, suggesting that kinetochore localization of 53BP1 is not mediated by phospho-H2AX. Further fine mapping studies will be necessary to clarify whether the same 53BP1 region initiates the recruitment of 53BP1 to DNA strand breaks or the kinetochore, respectively.

Phosphorylation by the ATM kinase plays a key role in the activation of various proteins involved in the DNA damage response (for example, see Ref. 22). A recent study by Bakkenist and Kastan (23) revealed that ATM forms an inactive oligomer in unirradiated cells. Upon radiation, ATM is rapidly autophosphorylated and dissociates from the complex thereby providing other substrates access to its kinase domain. Interestingly autophoshorylation and activation of ATM seem to occur at some distance to DNA break sites, and ATM then migrates in the nucleus to phosphorylate various substrates either at the break sites or elsewhere in the nucleus (23). This model is consistent with our finding that ATM-dependent phosphorylation of 53BP1 is not restricted to sites of DNA strand breaks and can occur within the entire nucleus. However, phosphorylation of 53BP1 alone is unlikely to trigger 53BP1 activation since deletion of the ATM target sites does not affect 53BP1 relocalization. Moreover the relocalization of 53BP1 appears to be required for efficient phosphorylation of ATM substrates at the sites of DNA breaks (data not shown). We therefore speculate that the rapid recruitment of 53BP1 to DNA break sites and the retention of 53BP1 at the sites of DNA breaks by binding to phospho-H2AX is one of the key steps in the activation of 53BP1 following DNA damage.

Acknowledgments—We thank Dr. Craig Bassing for the $H2AX^{Flox/Flox}$ and $H2AX^{\Delta/\Delta}$ ES cells. We also thank Drs. Larry Karnitz and Scott Kaufmann and members of the Chen and Karnitz laboratories for helpful discussions. We are grateful to the Mayo Protein Core facility for the synthesis of peptides and to the Mayo Gene Targeted Mouse Core facility for help with the generation of 53BP1-deficient mice and 53BP1-deficient ES cells.

REFERENCES

1. Iwabuchi, K., Bartel, P. L., Li, B., Marraccino, R., and Fields, S. (1994) *Proc. Natl. Acad. Sci. U. S. A.* **91,** 6098–6102
2. Iwabuchi, K., Li, B., Massa, H. F., Trask, B. J., Date, T., and Fields, S. (1998) *J. Biol. Chem.* **273,** 26061–26068
3. Rappold, I., Iwabuchi, K., Date, T., and Chen, J. (2001) *J. Cell Biol.* **153,** 613–620
4. Schultz, L. B., Chehab, N. H., Malikzay, A., and Halazonetis, T. D. (2000) *J. Cell Biol.* **151,** 1381–1390
5. Xia, Z., Morales, J. C., Dunphy, W. G., and Carpenter, P. B. (2000) *J. Biol. Chem.* **276,** 2708–2718
6. Anderson, L., Henderson, C., and Adachi, Y. (2001) *Mol. Cell. Biol.* **21,** 1719–1729
7. Bork, P., Hofmann, K., Bucher, P., Neuwald, A. F., Altschul, S. F., and Koonin, E. V. (1997) *FASEB J.* **11,** 68–76
8. Callebaut, I., and Mornon, J. P. (1997) *FEBS Lett.* **400,** 25–30
9. Yamane, K., Wu, X., and Chen, J. (2002) *Mol. Cell. Biol.* **22,** 555–566
10. DiTullio, R. A., Mochan, T. A., Venere, M., Bartkova, J., Sehested, M., Bartek, J., and Halazonetis, T. D. (2002) *Nat. Cell Biol.* **4,** 998–1002
11. Wang, B., Matsuoka, S., Carpenter, P. B., and Elledge, S. J. (2002) *Science* **298,** 1435–1438
12. Fernandez-Capetillo, O., Chen, H. T., Celeste, A., Ward, I., Romanienko, P. J., Morales, J. C., Naka, K., Xia, Z., Camerini-Otero, R. D., Motoyama, N., Carpenter, P. B., Bonner, W. M., Chen, J., and Nussenzweig, A. (2002) *Nat. Cell Biol.* **4,** 993–997
13. Ward, I. M., Minn, K., Van Deursen, J., and Chen, J. (2003) *Mol. Cell. Biol.* **23,** 2556–2563
14. Celeste, A., Petersen, S., Romanienko, P. J., Fernandez-Capetillo, O., Chen, H. T., Sedelnikova, O. A., Reina-San-Martin, B., Coppola, V., Meffre, E., Difilippantonio, M. J., Redon, C., Pilch, D. R., Olaru, A., Eckhaus, M., Camerini-Otero, R. D., Tessarollo, L., Livak, F., Manova, K., Bonner, W. M., Nussenzweig, M. C., and Nussenzweig, A. (2002) *Science* **296,** 922–927
15. Bassing, C. H., Chua, K. F., Sekiguchi, J., Suh, H., Whitlow, S. R., Fleming, J. C., Monroe, B. C., Ciccone, D. N., Yan, C., Vlasakova, K., Livingston, D. M., Ferguson, D. O., Scully, R., and Alt, F. W. (2002) *Proc. Natl. Acad. Sci. U. S. A.* **99,** 8173–8178
16. Cokol, M., Nair, R., and Rost, B. (2000) *EMBO Rep.* **1,** 411–415
17. Altschul, S. F., Madden, T. L., Schaffer, A. A., Zhang, J., Zhang, Z., Miller, W., and Lipman, D. J. (1997) *Nucleic Acids Res.* **25,** 3389–3402
18. Rogakou, E. P., Pilch, D. R., Orr, A. H., Ivanova, V. S., and Bonner, W. M. (1998) *J. Biol. Chem.* **273,** 5858–5868
19. Jullien, D., Vagnarelli, P., Earnshaw, W. C., and Adachi, Y. (2002) *J. Cell Sci.* **115,** 71–79
20. Yamane, K., Katayama, E., and Tsuruo, T. (2000) *Biochem. Biophys. Res. Commun.* **279,** 678–684
21. Morales, J. C., Xia, Z., Lu, T., Aldrich, M. B., Wang, B., Rosales, C., Kellems, R. E., Hittelman, W. N., Elledge, S. J., and Carpenter, P. B. (2003) *J. Biol. Chem.* **278,** 14971–14977
22. Abraham, R. T. (2001) *Genes Dev.* **15,** 2177–2196
23. Bakkenist, C. J., and Kastan, M. B. (2003) *Nature* **421,** 499–506

MOLECULAR AND CELLULAR BIOLOGY, Apr. 2003, p. 2556–2563
0270-7306/03/$08.00+0 DOI: 10.1128/MCB.23.7.2556–2563.2003

Vol. 23, No. 7

p53 Binding Protein 53BP1 Is Required for DNA Damage Responses and Tumor Suppression in Mice

Irene M. Ward,[1] Kay Minn,[1] Jan van Deursen,[2] and Junjie Chen[1]*

Departments of Oncology[1] and Pediatric and Adolescent Medicine,[2] Mayo Clinic and Foundation, Rochester, Minnesota 55905

Received 19 November 2002/Returned for modification 14 December 2002/Accepted 7 January 2003

53BP1 is a p53 binding protein of unknown function that binds to the central DNA-binding domain of p53. It relocates to the sites of DNA strand breaks in response to DNA damage and is a putative substrate of the ataxia telangiectasia-mutated (ATM) kinase. To study the biological role of 53BP1, we disrupted the 53BP1 gene in the mouse. We show that, similar to ATM$^{-/-}$ mice, 53BP1-deficient mice were growth retarded, immune deficient, radiation sensitive, and cancer prone. 53BP1$^{-/-}$ cells show a slight S-phase checkpoint defect and prolonged G_2/M arrest after treatment with ionizing radiation. Moreover, 53BP1$^{-/-}$ cells feature a defective DNA damage response with impaired Chk2 activation. These data indicate that 53BP1 acts downstream of ATM and upstream of Chk2 in the DNA damage response pathway and is involved in tumor suppression.

Defects in DNA damage recognition and repair mechanisms are associated with cancer predisposition. The tumor suppressor protein p53, a sequence specific transcription factor, plays a central role in the response of mammalian cells to genotoxic stress. 53BP1 (p53 binding protein 1) was cloned as a protein that interacts with the DNA-binding domain of p53 (13). It contains a tandem BRCT (BRCA1 C terminus) motif (5) with sequence homology to the tumor suppressor BRCA1 and DNA damage checkpoint protein scRad9. 53BP1 binds through the first of its C-terminal BRCT repeats and the inter-BRCT linker region to the central DNA-binding domain of p53 (7, 15) and has been shown to enhance p53-mediated transcription of reporter genes (14). More recently, in vitro studies suggest that 53BP1 participates in the cellular response to DNA damage. 53BP1 relocates to multiple nuclear foci within minutes after exposure of cells to ionizing radiation (IR) (2, 22, 23, 28). These foci colocalize with known DNA damage response proteins such as phosphorylated H2AX, Rad50/Mre11/NBS1, BRCA1, and Rad51 at sites of DNA lesions (2, 22, 23). 53BP1 becomes hyperphosphorylated in response to IR, and several lines of evidence suggest that 53BP1 is a downstream target of the ataxia telangiectasia-mutated (ATM) kinase, the product of the gene mutated in ataxia telangiectasia (2, 22, 28). Furthermore, 53BP1 localizes to kinetochores in mitotic cells, suggesting a potential function of 53BP1 in mitotic checkpoint signaling (16).

To study the biological function of 53BP1 in mammals, we created 53BP1-deficient mice. We report here that mice lacking 53BP1 are viable and display a phenotype that partially overlaps with that of ATM-deficient mice. 53BP1-deficient mice are growth retarded, immune deficient, radiation sensitive, and cancer prone. Thus, 53BP1 is required for an appropriate cellular response to DNA damage in vivo.

* Corresponding author. Mailing address: Department of Oncology, Mayo Clinic and Foundation, Rm. 1306, Guggenheim Bldg., 200 First St., SW, Rochester, MN 55905. Phone: (507) 538-1545. Fax: (507) 284-3906. E-mail: chen.junjie@mayo.edu.

MATERIALS AND METHODS

Gene targeting and generation of 53BP1-deficient mice. A mouse 53BP1 cDNA fragment was used as a probe to isolate 53BP1 mouse genomic DNA from a mouse 129 genomic DNA phage library (Stratagene). The genomic DNA was cloned into pZErO-2 (Invitrogen), and the exon-intron structure characterized by restriction digestion, Southern blotting, and DNA sequencing. The targeting vector was constructed by replacing the exon spanning nucleotides 3777 to 4048 of the mouse 53BP1 gene with the PGK-neo^r gene. The targeting vector was linearized and electroporated into 129/SvE embryonic stem (ES) cells. About 200 G418-resistant ES clones were screened by Southern blot analysis by using a probe that hybridizes to a 9.8-kb *Eco*RI restriction fragment in wild-type cells and an 8.3-kb fragment in homologous recombinants. Three independent ES clones with homologous integration at the targeting site were injected into C57BL/6 blastocysts to generate chimeric mice. These chimeras were subsequently crossed with C57BL/6 females, and heterozygous mice with successful germ line transmission of the targeted allele were used to generate 53BP1$^{-/-}$ mice.

Generation of 53BP1$^{-/-}$ MEFs and embryonic cells. Primary mouse embryonic fibroblasts (MEFs) were obtained from e14.5 embryos by a standard procedure. To generate 53BP1$^{-/-}$ embryonic cells, day 3 blastocytes from $-/-$ matings were isolated and an embryonic cell line was established by a standard procedure.

Proliferation and clonogenic assays. MEFs from three 53BP1$^{-/-}$ and three genetically matched 53BP1$^{+/+}$ embryos were plated at a density of 10^5 cells/well in six-well plates. Every day one set of cells was treated with trypsin and counted. At days 3 and 6, cells were split and replated into larger dishes. For the clonognic cell survival assay, 53BP1$^{-/-}$ and 53BP1$^{+/+}$ embryonic cells were plated into 60-by-15-mm dishes and 6 h later exposed to different doses of IR. After 7 days of culture, the number of colonies was counted.

Western blot and immunofluorescence analysis. Western blot analyses were performed by a standard procedure. Immunofluorescence staining was performed as described previously (26). Antibodies against 53BP1, Chk2, Chk2T68P, and γ-H2AX were generated as described previously (22, 26, 27). The antibodies to p53 (FL393G) and actin were purchased from Santa Cruz and Sigma, respectively. The antibodies to mouse NBS1 and BRCA1 were gifts from A. Nussenzweig and L. Chodosh, respectively.

Cell cycle checkpoints and flow cytometry analysis. For analysis of G_2/M checkpoint function, MEFs from 53BP1$^{-/-}$ and genetically matched 53BP1$^{+/+}$ embryos, as well as ES cells, were irradiated with different doses of IR and stained 1 h later with anti-P-Histone 3 (Upstate). Aliquots of the cells were also labeled with bromodeoxyuridine (BrdU) for 1 h before exposure to 6 Gy of IR, harvested at different time points after IR, and stained with anti-BrdU-FITC (Becton Dickinson) and propidium iodide. To monitor radiation-induced inhibition of DNA synthesis, MEFs were labeled for 48 h with 20 nCi of [^{14}C]thymidine ml^{-1} before exposure to 0 or 20 Gy of IR. At 30 min after IR cells were pulse-labeled for 30 min with 2.5 mCi of [^{3}H]thymidine ml^{-1} and harvested. Radioactivity was measured in a liquid scintillation counter.

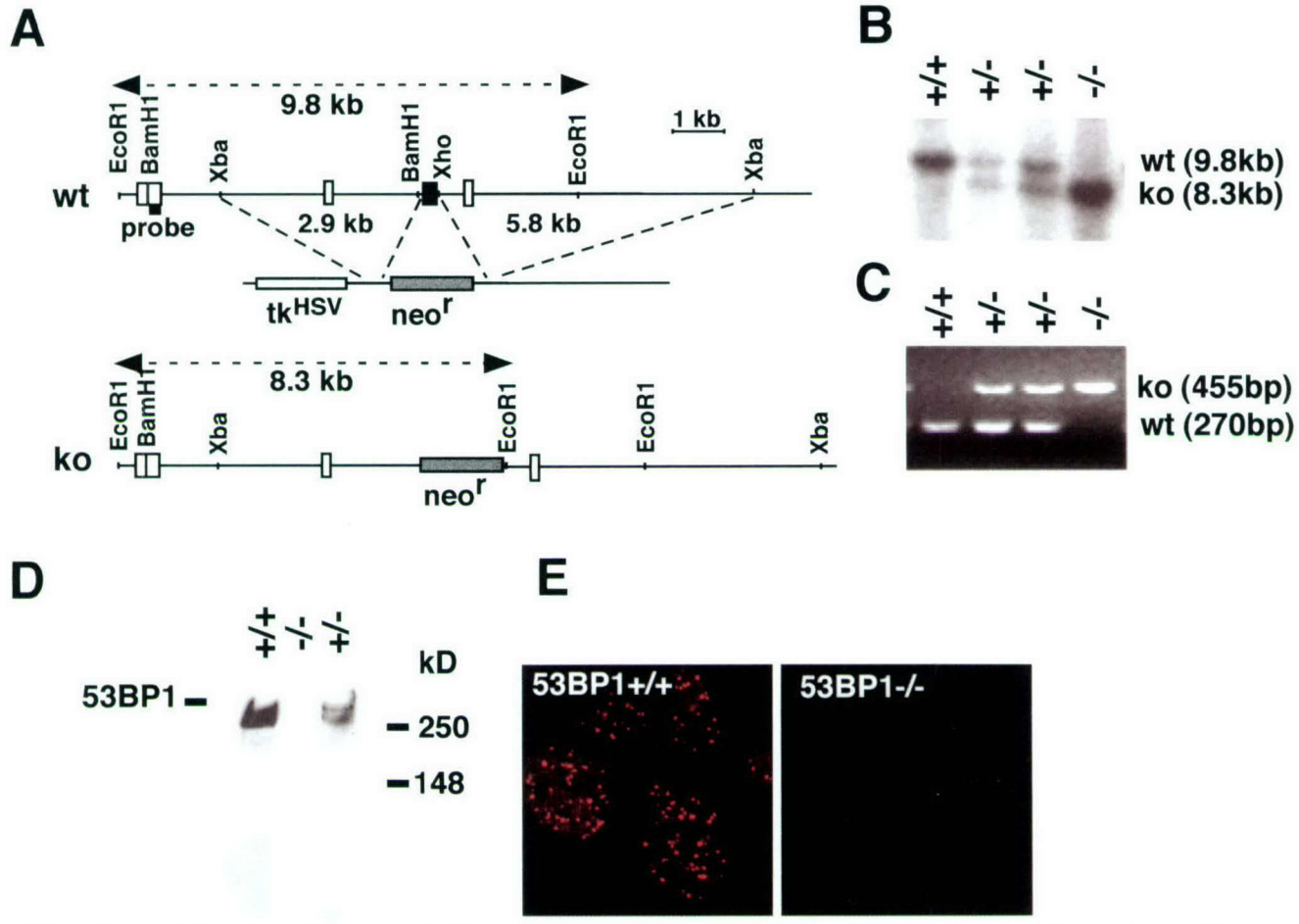

FIG. 1. Targeted disruption of the mouse 53BP1 gene. (A) Map of the genomic locus surrounding the targeted exon, the targeting vector containing the PGK-neo cassette, and the targeted locus. A 5′-flanking probe used for screening ES cell clones and mice is indicated. (B) Southern blot analysis of *Eco*RI-digested genomic DNA. (C) Multiplex PCR genotype analysis with a primer pair for the *neo* gene (resulting in a 455-bp product) and a 5′ external exon (resulting in a 270-bp product). (D) Western blot of cell extracts from mouse testes with an antibody specific for the N terminus of 53BP1. (E) Immunofluorescence analysis of irradiated (1 Gy) $53BP1^{+/+}$ and $53BP1^{-/-}$ MEFs with polyclonal antibodies raised against the N terminus of 53BP1.

Thymocytes, white blood cells, and tumor cells were stained with anti-CD4-phycoerythrin and anti-CD8-fluorescein isothiocyanate or the respective isotype controls (all from Pharmingen) and then analyzed on a flow cytometer.

Histopathological analysis and chromosome spreads. Tissues were collected and fixed in 10% buffered formalin or Bouin's fixative, embedded in paraffin blocks, sectioned, and stained with hematoxylin-eosin. Metaphase spreads were prepared by a standard procedure.

RESULTS

Phenotype of 53BP1-deficient mice. To analyze the physiological role of 53BP1 in mammalian cells, we generated 53BP1-deficient mice. The targeting vector was constructed by replacing the exon spanning nucleotides 3777 to 4048 of the mouse 53BP1 cDNA with the PGK-neo^r gene (Fig. 1A to C). $53BP1^{-/-}$ mice were viable and born at ratios close to the expected Mendelian proportion (25% [+/+], 52% [+/−], and 23% [−/−]). The complete absence of 53BP1 protein was confirmed by Western blot and immunofluorescence analyses with antibodies raised against the N terminus of 53BP1 (Fig. 1D and E).

Since 53BP1 is a putative substrate of ATM in the DNA damage response pathway, we examined whether $53BP1^{-/-}$ mice show a similar phenotype as ATM-deficient mice. $ATM^{-/-}$ mice are growth retarded and ATM-deficient fibroblasts grow poorly in culture (3, 9, 30). Similarly, $53BP1^{-/-}$ mice are significantly smaller than their +/+ and +/− littermates (male, 38.29 ± 3.6 g [+/+], 28.28 ± 3.5 g [−/−], and 34.91 ± 2.6 g [+/−]; female, 29.38 ± 4.8 g [+/+], 23.85 ± 3.1 g [−/−], and 27.89 ± 3.5g [+/−]; also see Fig. 2A). Consistent with this finding, MEFs derived from E14.5 null embryos showed a lower proliferation rate than genetically matched wild-type controls (data not shown). ATM-deficient mice are infertile due to meiotic failure (3, 9, 30). In contrast, both male and female 53BP1-deficient mice were fertile, although the average litter size of $53BP1^{-/-}$ intercrosses was slightly reduced compared to 53BP1-wild-type intercrosses (data not shown). Histological examination of the testes revealed no overt defect in spermatogenesis, suggesting that 53BP1 plays no apparent role in meiosis.

Cell cycle checkpoint regulation in $53BP1^{-/-}$ cells. ATM-deficient cells exhibit a defect in the G_2/M checkpoint and do

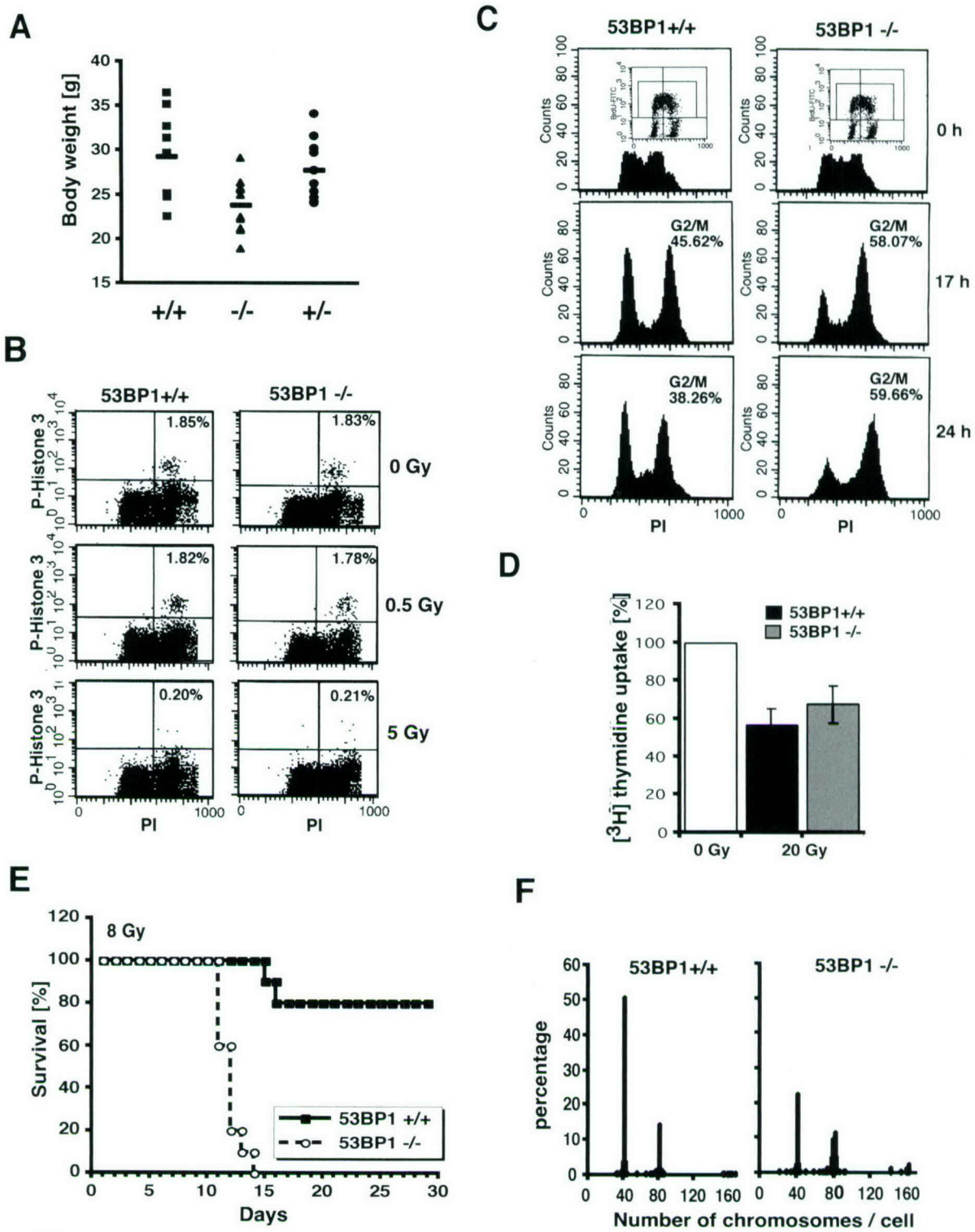

FIG. 2. 53BP1 deficiency results in growth retardation, cell cycle defect, radiosensitivity, and chromosomal instability. (A) Body weights of female 53BP1 wild-type, heterozygous, and knockout mice at 5 months of age. (B) G_2/M arrest of $53BP1^{+/+}$ and $53BP1^{-/-}$ embryonic cells in response to 0.5 or 5 Gy of IR. Cells were stained with anti-P-Histone 3 antibody 1 h after IR and analyzed by fluorescence-activated cell sorting. (C) G_2 accumulation of $53BP1^{+/+}$ and $53BP1^{-/-}$ MEFs several hours after IR. Cells were pulse-labeled for 1 h with BrdU before exposure to 6 Gy of IR. The cell cycle profile of BrdU-positive cells was analyzed by staining with propidium iodide. Consistent data were obtained in three independent experiments. (D) IR-induced intra-S-phase checkpoint in $53BP1^{+/+}$ and $53BP1^{-/-}$ MEFs. DNA synthesis was assessed by [3H]thymidine incorporation 30 min after exposure to 20 Gy of IR. (E) Sensitivity of 10 pairs of female $53BP1^{-/-}$ and $53BP1^{+/+}$ littermates to 8 Gy of whole body IR. Similar results were observed with 10 male pairs. (F) Chromosomal instability in $53BP1^{-/-}$ MEFs. 100 metaphase spreads from genetically matched passage three $53BP1^{+/+}$ and $53BP1^{-/-}$ MEFs were analyzed. Consistent data were obtained from three different experiments.

not arrest in G_2 in the first 2 h after IR (for example, see reference 29). However, flow cytometric analysis of phospho-H3-positive mitotic embryonic cells revealed no apparent G_2/M checkpoint defect in 53BP1$^{-/-}$ cells in response to different doses of IR (Fig. 2B and data not shown).

Several hours after IR, ATM-deficient cells show a prolonged accumulation in G_2/M (29). A similar phenotype was observed in 53BP1$^{-/-}$ fibroblasts. As shown in Fig. 2C, irradiated 53BP1-null cells, like 53BP1$^{+/+}$ cells, were arrested in G_2 but showed a delayed exit from the G_2/M phase. Consistent with 53BP1$^{-/-}$ cells arrested at the G_2 phase, the percentage of mitotic cells 24 h after IR was approximately three times lower in nocodazole-treated 53BP1$^{-/-}$ cells than in 53BP1 wild-type cells, as assessed by immunostaining with anti-phospho-histone H3 antibodies (data not shown).

Cells derived from ataxia telangiectasia patients show a defect in the IR-induced G_1 delay (18). In contrast, 53BP1-deficient MEFs, synchronized by a cycle of serum starvation and release, exhibited a normal G_1 arrest in response to 10 to 20 Gy of IR (data not shown).

ATM-deficient cells also feature a defect in the intra-S phase checkpoint, resulting in a radioresistant DNA synthesis phenotype (3). Both 53BP1$^{+/+}$ and 53BP1$^{-/-}$ fibroblasts showed inhibition of DNA synthesis in response to 20 Gy of IR, although the response was slightly impaired in 53BP1$^{-/-}$ cells (Fig. 2D).

Thus, although 53BP1 may play a subtle role in intra-S-phase regulation, it appears not to be critical for G_1 or early G_2/M checkpoint control.

Radiosensitivity of 53BP1$^{-/-}$ mice and cells. Another hallmark of ATM-deficiency is extreme radiation sensitivity (for example, see reference 3). Similarly, 53BP1$^{-/-}$ mice showed a marked hypersensitivity to whole-body irradiation. All 53BP1$^{-/-}$ mice died by 14 days after exposure to 8 Gy of IR, whereas the majority of 53BP1$^{+/+}$ mice were viable for at least 2 months after irradiation (Fig. 2E). Necroptic examination revealed radiation-induced intestinal bleeding and bone marrow failure as the cause of death (data not shown). Consistent with this finding, in vitro clonogenic survival assays with embryonic cells indicated a two- to threefold-higher radiation sensitivity in 53BP1-deficient cells than in 53BP1-wild-type cells, although the difference was less dramatic than in vivo (data not shown).

Chromosomal instability of 53BP1$^{-/-}$ cells. To determine whether loss of 53BP1 causes chromosomal instability, another characteristic of ATM$^{-/-}$ cells, we examined metaphase spreads of passage 3 53BP1$^{-/-}$ and 53BP1$^{+/+}$ MEFs. Unlike ATM-deficient cells, 53BP1$^{-/-}$ fibroblasts showed no spontaneous chromosomal breaks. However, we observed a tendency toward aneuploidy and/or tetraploidy in 53BP1-null cells, suggesting a possible defect in chromosome segregation (Fig. 2F).

Immunodeficiency and thymic lymphomas in 53BP1$^{-/-}$ mice. ATM$^{-/-}$ mice show various immune defects, including reduced numbers of pre-B cells, thymocytes, and peripheral T cells, and develop malignant thymic lymphomas by between 2 and 4 months of age (3, 9, 30). We therefore sought to determine whether the loss of 53BP1 might be accompanied by immunological abnormalities and predisposition to tumor formation. Indeed, thymus cellularity in 53BP1$^{-/-}$ mice was reduced by 40% compared to wild-type littermates. Immunophenotyping of 6-week-old mice revealed an approximately twofold reduction in the percentage of CD4$^+$ mature thymocytes (with absolute average numbers of 7×10^6 cells in 53BP1$^{+/+}$ mice and 2.8×10^6 cells in 53BP1$^{-/-}$ mice) accompanied by a maximum twofold increase in the percentage of CD4$^-$ CD8$^-$ progenitors. CD4$^+$ T lymphocytes in the peripheral blood of 53BP1$^{-/-}$ mice were also reduced by approximately twofold (with absolute average numbers of 8.2×10^5 cells/ml in 53BP1$^{-/-}$ mice and 16.9×10^5 cells/ml in 53BP1$^{+/+}$ mice). Furthermore, of 101 53BP1$^{-/-}$ mice, 8 developed massive thymic lymphomas with or without infiltration of the lymph nodes, spleen, and kidney at the ages of 4 to 7 months (Fig. 3A to C). Flow cytometric analysis of three of these tumors revealed a CD4$^+$ CD8$^+$ immunophenotype (Fig. 3A and data not shown). Although the tumor frequency in 53BP1$^{-/-}$ mice is much lower than in ATM$^{-/-}$ mice (8% versus 100%), it is highly significant since none of the 53BP1$^{+/+}$ and 53BP1$^{+/-}$ mice ($n = 54$ and $n = 97$, respectively) developed any tumors over the same time period. In addition to the eight 53BP1$^{-/-}$ mice with malignant lymphomas, nine more 53BP1$^{-/-}$ mice died at the ages of 1 to 7 months without overt detectable tumors (Fig. 3D). Given the chronic immunosuppression of 53BP1$^{-/-}$ mice, it is possible that some of these deaths might be due to overwhelming opportunistic infections. Among the control animals, only one 53BP1$^{+/+}$ mouse and two 53BP1$^{+/-}$ miced died of unidentified reasons (Fig. 3D).

Role of 53BP1 in DNA damage signaling pathway. The partially overlapping phenotypes of 53BP1- and ATM-deficient mice support the hypothesis that 53BP1 acts downstream of ATM in the DNA damage pathway. ATM becomes activated in response to irradiation and phosphorylates numerous downstream targets, including H2AX, NBS1, Chk2, and p53, that mediate cell cycle checkpoint control and DNA repair (for example, see reference 1). To obtain a better understanding of the complex organization of this pathway, we examined the effect of 53BP1 deficiency on the activation of some of these downstream targets.

We have shown earlier that 53BP1 associates with γ-H2AX within minutes after exposure to IR (22), thus raising the possibility that γ-H2AX may be required for the recruitment of 53BP1. Indeed, 53BP1 foci are not observed in H2AX-deficient cells (6). Consistent with this model, γ-H2AX foci formation was found normal in 53BP1$^{-/-}$ MEFs (Fig. 4A), suggesting that 53BP1 acts downstream of ATM and H2AX. Since H2AX is also required for the localization of NBS1 to the sites of DNA breaks (6, 21), we examined whether any of these events are 53BP1 dependent. As shown in Fig. 4A, radiation-induced NBS1 foci formation appears to be normal in 53BP1$^{-/-}$ cells, suggesting that 53BP1 is not required for the recruitment of NBS1 to sites of DNA strand breaks.

Chk2 is another downstream effector of ATM. Chk2 is activated after IR and contributes to the IR-induced checkpoint control by phosphorylating several substrates including Cdc25C, Cdc25A, BRCA1, and p53 (4). ATM phosphorylates Chk2 at Thr-68 in response to IR, and this phosphorylation event is required for the full activation of Chk2 kinase (19, 20). Coimmunoprecipitation analyses demonstrate an interaction between 53BP1 and Chk2 in undam-

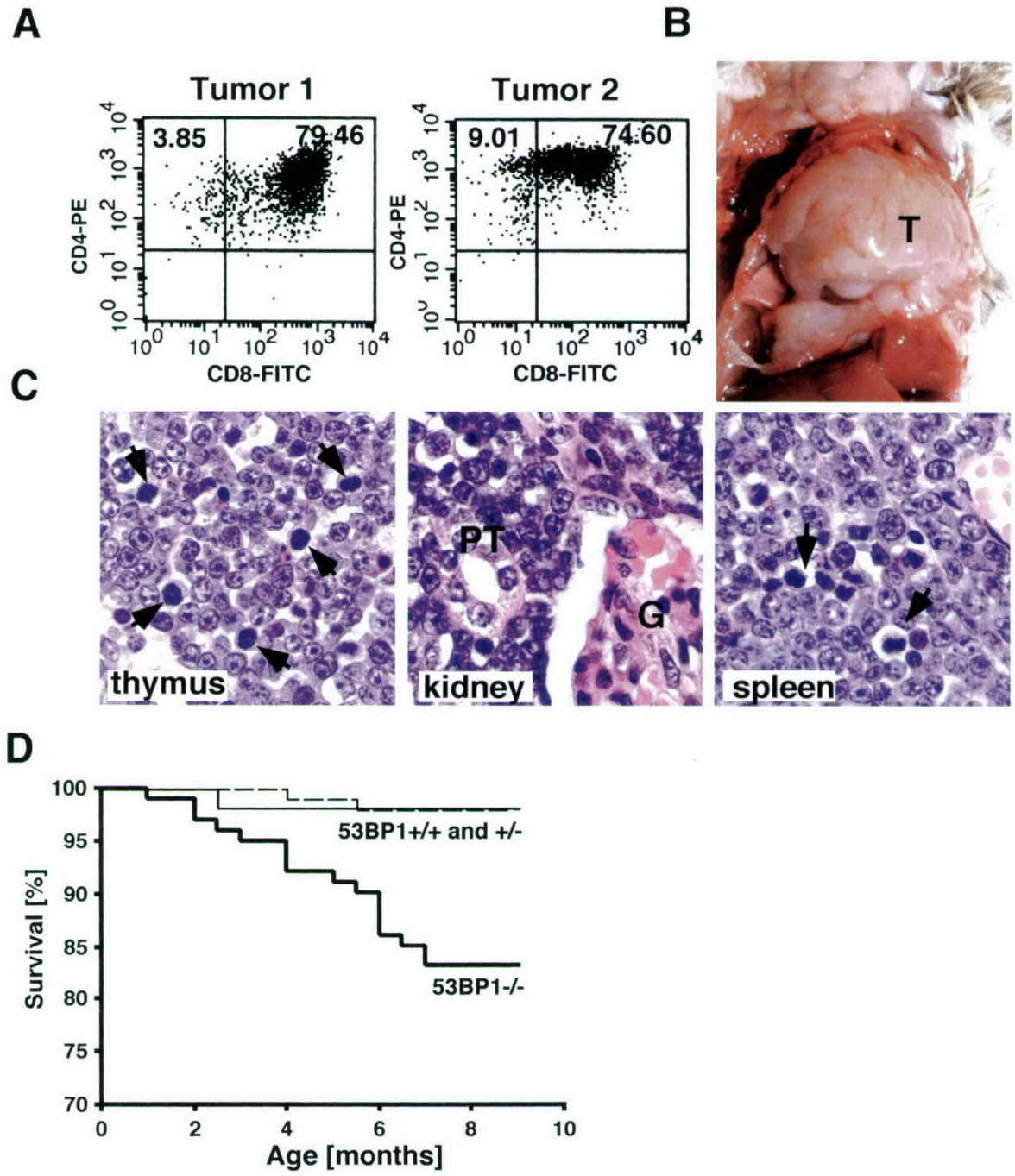

FIG. 3. 53BP1$^{-/-}$ mice are tumor prone. (A) CD4 and CD8 cell surface expression of cells from two different thymic lymphomas was assessed by flow cytometry. (B) Massive thymic lymphoma (T) in a 4-month-old 53BP1$^{-/-}$ mouse. (C) Hematoxylin-and-eosin-stained sections from the thymus, spleen, and kidney of a 53BP1$^{-/-}$ animal with thymic lymphoma. Monomorphic lymphoblastic tumor cells are dominant in all three tissues. The arrows indicate mitotic figures. G, glomerulus; PT, proximal tubulus. (D) Overall survival of 53BP1$^{+/+}$ (n = 54), 53BP1$^{+/-}$ (n = 97), and 53BP1$^{-/-}$ (n = 101) mice over a period of 10 months.

aged cells (Fig. 4B). Interestingly, this interaction decreases after IR (Fig. 4B). Since we have shown earlier that the activated form of Chk2 localizes in distinct foci at the sites of DNA lesions (27), we first examined the focus formation of phospho-Chk2. In these experiments, we used a guinea pig anti-Chk2T68P antibody that specifically recognizes Chk2 in Chk2$^{+/+}$ cells but not in Chk2$^{-/-}$ cells (Fig. 4G). As shown in Fig. 4C, focus formation of phosphorylated Chk2 (Chk2T68P) was abolished in 53BP1$^{-/-}$ MEFs upon exposure to 1 Gy of IR. Furthermore, Chk2 phosphorylation, as assessed by gel mobility shift, was reduced in 53BP1$^{-/-}$ MEFs in response to low doses of radiation (≤5 Gy, Fig. 4E

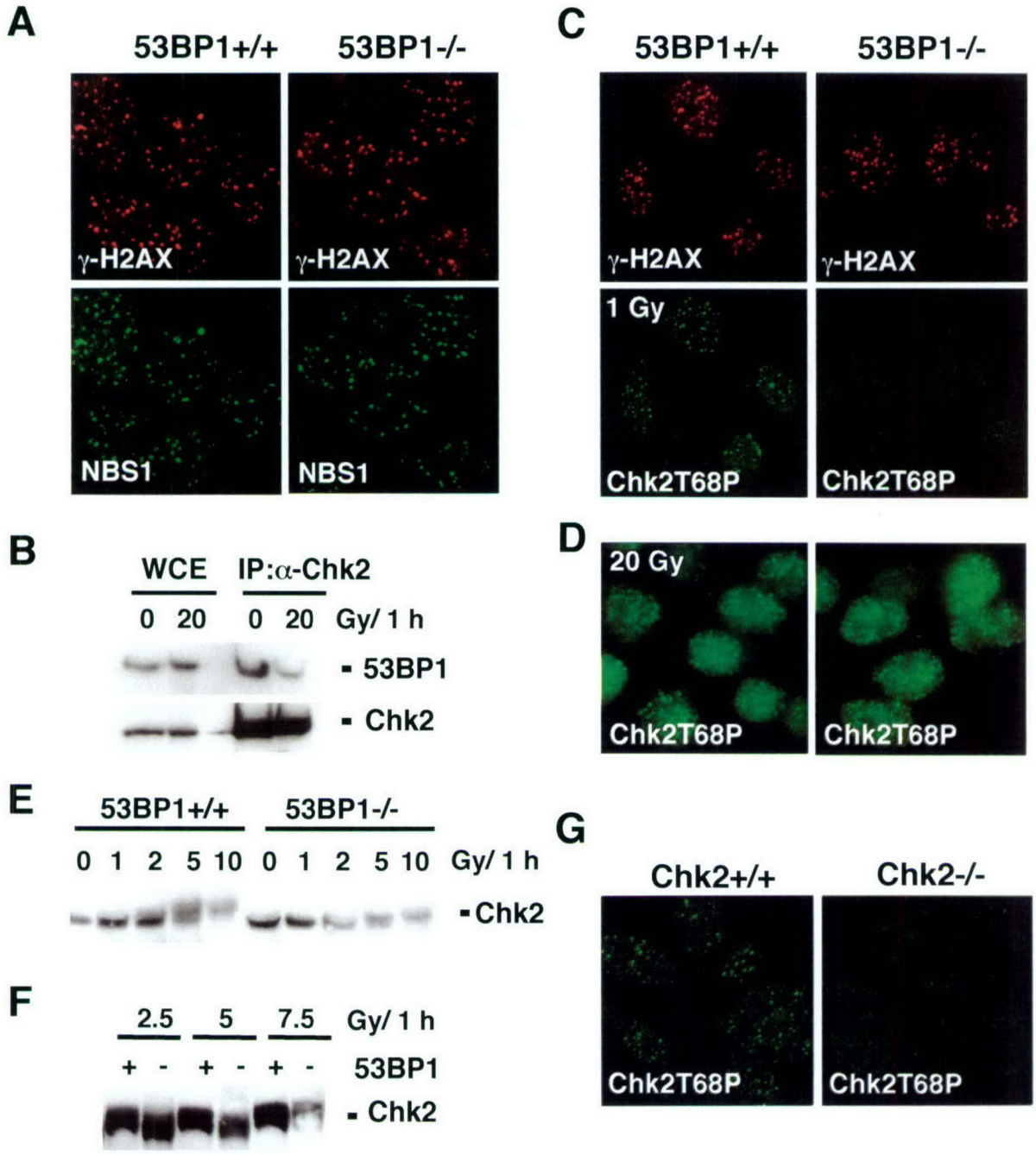

FIG. 4. Irradiated 53BP$^{-/-}$ MEFs show impaired Chk2 activation after low doses of IR. (A) γ-H2AX and NBS1 focus formation 6 h after exposure to 6 Gy of IR is unaffected in 53BP1$^{-/-}$MEFs compared to 53BP1 wild-type MEFs, as assessed by immunofluorescence staining. (B) Coimmunoprecipitation of 53BP1 and Chk2 in untreated or irradiated 293T cells. (C) Activated Chk2 phosphorylated at Thr 68 (Chk2T68) forms foci in 53BP1$^{+/+}$ MEFs 1 h after exposure to 1 Gy of IR. No foci are detectable in 53BP1$^{-/-}$ MEFs at this low dose of IR. γ-H2AX staining is shown as a control. (D) Chk2T68P foci form in both 53BP1$^{+/+}$ and 53BP1$^{-/-}$ cells in response to 20 Gy of IR. (E) Chk2 mobility shift is reduced in 53BP1$^{-/-}$ MEFs in response to low-dose radiation. Cell lysates from 53BP1$^{+/+}$ and 53BP1$^{-/-}$ MEFs were prepared 1 h after IR and immunoblotted with anti-Chk2 antibody. (F) For better comparison of the Chk2 mobility shift, lysates from irradiated 53BP1$^{+/+}$ and 53BP1$^{-/-}$ cells were run side by side. (G) The guinea pig anti-Chk2T68P antibody specifically recognizes Chk2.

and F). However, no difference in Chk2T68 focus formation or Chk2 mobility shift was observed at high doses of IR (Fig. 4D and F and data not shown). These findings suggest that 53BP1 is required for optimal activation of Chk2 after low doses of IR.

DISCUSSION

By disrupting the 53BP1 gene, we generated mice that lack 53BP1 protein. 53BP1-deficient mice are growth retarded, immunocompromised, and highly radiation sensitive. Further-

more, 8 of 101 53BP1$^{-/-}$ mice developed lymphoid tumors at 4 to 7 months of age. Cells derived from 53BP1-deficient mice show a tendency to genetic instability and feature a defective DNA damage response with impaired Chk2 activation. Thus, 53BP1 is likely to be required for the cellular response to DNA damage, although its precise role remains to be resolved.

We did not observe any marked cell cycle checkpoint defects in 53BP1-deficient cells. B cells from 53BP1$^{-/-}$ mice (11), as well as human cell lines treated with small interfering RNA directed against 53BP1, show an impaired early G_2M checkpoint in response to low-dose IR (25). However, we failed to detect this defect in 53BP1$^{-/-}$ mouse embryonic cells. This discrepancy may be due to tissue-specific functions of 53BP1 since the experiments were performed with different types of cells or cell lines. Similarly, H2AX$^{-/-}$ B cells show a clearly impaired early G_2M checkpoint, whereas the defect is very minor in H2AX$^{-/-}$ MEFs (11).

The prolonged G_2 arrest observed several hours after exposure to IR is unlikely to represent a checkpoint defect but rather reflects an impaired ability to repair DNA double-strand breaks (DSBs) prior to progressing through the cell cycle. This idea is supported by the hypersensitivity of 53BP1-deficient mice to IR. Mammalian cells are thought to repair DNA DSBs primarily by nonhomologous end joining (17). Homologous recombination, the predominant DSB repair pathway in bacteria and yeast, appears to have a minor contribution to the repair of IR in adult mice, although it plays a major role during DNA replication in embryos (10). The IR hypersensitivity observed in adult 53BP1$^{-/-}$ mice, together with a moderate IR sensitivity seen in embryonic cells, points to a defect in the DNA end-joining pathway. However, further experiments need to be conducted to resolve the precise repair defects in 53BP1-deficient cells.

One important function of DNA end joining lies in the processing of RAG1/2-induced DSBs that arise during the rearrangement of V(D)J segments in T-cell receptor and immunoglobulin genes (10). Unrepaired RAG-induced DSBs can initiate translocations that lead to oncogenic gene amplification and transformation (8, 31). 53BP1-deficient mice exhibit immunological abnormalities and an increased risk of developing lymphomas. We speculate that 53BP1$^{-/-}$ lymphomas arise from an inability to detect or repair abnormal V(D)J recombination, although further studies are necessary to clarify the underlying mechanism of lymphoma development in 53BP1-deficient mice.

53BP1-deficient cells exhibit a defect in Chk2 activation in response to low-dose IR. Interestingly, the phenotype of Chk2$^{-/-}$ mice is very different from that of 53BP1$^{-/-}$ mice. Chk2-deficient mice show reduced sensitivity to IR, and Chk2$^{-/-}$ thymocytes exhibit resistance to IR-induced apoptosis (12, 24). In contrast, 53BP1$^{-/-}$ mice are IR hypersensitive and 53BP1$^{-/-}$ thymocytes show increased IR-induced apoptosis (unpublished observations). These differences indicate that the phenotype of 53BP1-deficient mice or cells is not primarily mediated by Chk2, although 53BP1 is required for optimal Chk2 activation in response to low-dose IR.

Taken together, our data demonstrate that 53BP1 plays a role early in the DNA damage response pathway. 53BP1 acts downstream of ATM and H2AX and participates in a subset of ATM functions. 53BP1 is required for optimal activation of Chk2 in response to low doses of IR. More importantly, loss of 53BP1 leads to radiation sensitivity and tumorigenesis in mice, further supporting the hypothesis that defects in DNA damage responses contribute to tumorigenesis in mammals.

ACKNOWLEDGMENTS

We thank Andre Nussenzweig, Lewis Chodosh, Xiaohua Wu, Shirdar Ganesan, and David Livingston for valuable reagents and Larry Karnitz, Scott Kaufmann, and members of the Chen and Karnitz laboratories for helpful discussions. We are grateful to the Mayo Protein Core facility for synthesis of peptides and the Mayo Monoclonal Core facility for help in antibody production.

This work was supported by grants from National Institute of Health, the Breast Cancer Research Foundation, and Prospect Creek Foundation. J.C. is a recipient of DOD breast cancer career development award. I.W. is supported by a postdoctoral fellowship from the DOD Breast Cancer Research program.

REFERENCES

1. **Abraham, R. T.** 2001. Cell cycle checkpoint signaling through the ATM and ATR kinases. Genes Dev. **15:**2177–2196.
2. **Anderson, L., C. Henderson, and Y. Adachi.** 2001. Phosphorylation and rapid relocalization of 53BP1 to nuclear foci upon DNA damage. Mol. Cell. Biol. **21:**1719–1729.
3. **Barlow, C., S. Hirotsune, R. Paylor, M. Liyanage, M. Eckhaus, F. Collins, Y. Shiloh, J. N. Crawley, T. Ried, D. Tagle, and A. Wynshaw-Boris.** 1996. ATM-deficient mice: a paradigm of ataxia telangiectasia. Cell **86:**159–171.
4. **Bartek, J., J. Falck, and J. Lukas.** 2001. CHK2 kinase: a busy messenger. Nat. Rev. Mol. Cell. Biol. **2:**877–886.
5. **Callebaut, I., and J. P. Mornon.** 1997. From BRCA1 to RAP1: a widespread BRCT module closely associated with DNA repair. FEBS Lett. **400:**25–30.
6. **Celeste, A., S. Petersen, P. J. Romanienko, O. Fernandez-Capetillo, H. T. Chen, O. A. Sedelnikova, B. Reina-San-Martin, V. Coppola, E. Meffre, M. J. Difilippantonio, C. Redon, D. R. Pilch, A. Olaru, M. Eckhaus, R. D. Camerini-Otero, L. Tessarollo, F. Livak, K. Manova, W. M. Bonner, M. C. Nussenzweig, and A. Nussenzweig.** 2002. Genomic instability in mice lacking histone H2AX. Science **296:**922–927.
7. **Derbyshire, D. J., B. P. Basu, L. C. Serpell, W. S. Joo, T. Date, K. Iwabuchi, and A. J. Doherty.** 2002. Crystal structure of human 53BP1 BRCT domains bound to p53 tumour suppressor. EMBO J. **21:**3863–3872.
8. **Difilippantonio, M. J., S. Petersen, H. T. Chen, R. Johnson, M. Jasin, R. Kanaar, T. Ried, and A. Nussenzweig.** 2002. Evidence for replicative repair of DNA double-strand breaks leading to oncogenic translocation and gene amplification. J. Exp. Med. **196:**469–480.
9. **Elson, A., Y. Wang, C. J. Daugherty, C. C. Morton, F. Zhou, J. Campos-Torres, and P. Leder.** 1996. Pleiotropic defects in ataxia-telangiectasia protein-deficient mice. Proc. Natl. Acad. Sci. USA **93:**13084–13089.
10. **Essers, J., H. van Steeg, J. de Wit, S. M. Swagemakers, M. Vermeij, J. H. Hoeijmakers, and R. Kanaar.** 2000. Homologous and non-homologous recombination differentially affect DNA damage repair in mice. EMBO J. **19:**1703–1710.
11. **Fernandez-Capetillo, O., H. T. Chen, A. Celeste, I. Ward, P. J. Romanienko, J. C. Morales, K. Naka, Z. Xia, R. D. Camerini-Otero, N. Motoyama, P. B. Carpenter, W. M. Bonner, J. Chen, and A. Nussenzweig.** 2002. DNA damage-induced G_2-M checkpoint activation by histone H2AX and 53BP1. Nat. Cell Biol. **4:**993–997.
12. **Hirao, A., A. Cheung, G. Duncan, P. M. Girard, A. J. Elia, A. Wakeham, H. Okada, T. Sarkissian, J. A. Wong, T. Sakai, E. De Stanchina, R. G. Bristow, T. Suda, S. W. Lowe, P. A. Jeggo, S. J. Elledge, and T. W. Mak.** 2002. Chk2 is a tumor suppressor that regulates apoptosis in both an ataxia telangiectasia mutated (ATM)-dependent and an ATM-independent manner. Mol. Cell. Biol. **22:**6521–6532.
13. **Iwabuchi, K., P. L. Bartel, B. Li, R. Marraccino, and S. Fields.** 1994. Two cellular proteins that bind to wild-type but not mutant p53. Proc. Natl. Acad. Sci. USA **91:**6098–6102.
14. **Iwabuchi, K., B. Li, H. F. Massa, B. J. Trask, T. Date, and S. Fields.** 1998. Stimulation of p53-mediated transcriptional activation by the p53-binding proteins, 53BP1 and 53BP2. J. Biol. Chem. **273:**26061–26068.
15. **Joo, W. S., P. D. Jeffrey, S. B. Cantor, M. S. Finnin, D. M. Livingston, and N. P. Pavletich.** 2002. Structure of the 53BP1 BRCT region bound to p53 and its comparison to the Brca1 BRCT structure. Genes Dev. **16:**583–593.
16. **Jullien, D., P. Vagnarelli, W. C. Earnshaw, and Y. Adachi.** 2002. Kinetochore localisation of the DNA damage response component 53BP1 during mitosis. J. Cell Sci. **115:**71–79.
17. **Kanaar, R., J. H. Hoeijmakers, and D. C. van Gent.** 1998. Molecular mechanisms of DNA double strand break repair. Trends Cell Biol. **8:**483–489.
18. **Khanna, K. K., H. Beamish, J. Yan, K. Hobson, R. Williams, I. Dunn, and**

M. F. Lavin. 1995. Nature of G_1/S cell cycle checkpoint defect in ataxia-telangiectasia. Oncogene **11:**609–618.

19. **Matsuoka, S., G. Rotman, A. Ogawa, Y. Shiloh, K. Tamai, and S. J. Elledge.** 2000. Ataxia telangiectasia-mutated phosphorylates Chk2 in vivo and in vitro. Proc. Natl. Acad. Sci. USA **97:**10389–10394.
20. **Melchionna, R., X. B. Chen, A. Blasina, and C. H. McGowan.** 2000. Threonine 68 is required for radiation-induced phosphorylation and activation of Cds1. Nat. Cell Biol. **2:**762–765.
21. **Paull, T. T., E. P. Rogakou, V. Yamazaki, C. U. Kirchgessner, M. Gellert, and W. M. Bonner.** 2000. A critical role for histone H2AX in recruitment of repair factors to nuclear foci after DNA damage. Curr. Biol. **10:**886–895.
22. **Rappold, I., K. Iwabuchi, T. Date, and J. Chen.** 2001. Tumor suppressor p53 binding protein 1 (53BP1) is involved in DNA damage-signaling pathways. J. Cell Biol. **153:**613–620.
23. **Schultz, L. B., N. H. Chehab, A. Malikzay, and T. D. Halazonetis.** 2000. p53 binding protein 1 (53BP1) is an early participant in the cellular response to DNA double-strand breaks. J. Cell Biol. **151:**1381–1390.
24. **Takai, H., K. Naka, Y. Okada, M. Watanabe, N. Harada, S. Saito, C. W. Anderson, E. Appella, M. Nakanishi, H. Suzuki, K. Nagashima, H. Sawa, K. Ikeda, and N. Motoyama.** 2002. Chk2-deficient mice exhibit radioresistance and defective p53-mediated transcription. EMBO J. **21:**5195–5205.
25. **Wang, B., S. Matsuoka, P. B. Carpenter, and S. J. Elledge.** 2002. 53BP1, a mediator of the DNA damage checkpoint. Science **283:**1435–1438.
26. **Ward, I. M., and J. Chen.** 2001. Histone H2AX is phosphorylated in an ATR-dependent manner in response to replicational stress. J. Biol. Chem. **276:**47759–47762.
27. **Ward, I. M., X. Wu, and J. Chen.** 2001. Threonine 68 of Chk2 is phosphorylated at sites of DNA strand breaks. J. Biol. Chem. **276:**47755–47758.
28. **Xia, Z., J. C. Morales, W. G. Dunphy, and P. B. Carpenter.** 2001. Negative cell cycle regulation and DNA damage inducible phosphorylation of the BRCT protein 53BP1. J. Biol. Chem. **276:**2708–2718.
29. **Xu, B., S. T. Kim, D. S. Lim, and M. B. Kastan.** 2002. Two molecularly distinct G_2/M checkpoints are induced by ionizing irradiation. Mol. Cell. Biol. **22:**1049–1059.
30. **Xu, Y., T. Ashley, E. E. Brainerd, R. T. Bronson, M. S. Meyn, and D. Baltimore.** 1996. Targeted disruption of ATM leads to growth retardation, chromosomal fragmentation during meiosis, immune defects, and thymic lymphoma. Genes Dev. **10:**2411–2422.
31. **Zhu, C., K. D. Mills, D. O. Ferguson, C. Lee, J. Manis, J. Fleming, Y. Gao, C. C. Morton, and F. W. Alt.** 2002. Unrepaired DNA breaks in p53-deficient cells lead to oncogenic gene amplification subsequent to translocations. Cell **109:**811–821.

JCB Report

53BP1 is required for class switch recombination

Irene M. Ward,[1] Bernardo Reina-San-Martin,[4] Alexandru Olaru,[5] Kay Minn,[1] Koji Tamada,[2] Julie S. Lau,[2] Marilia Cascalho,[3] Lieping Chen,[2] Andre Nussenzweig,[6] Ferenc Livak,[5] Michel C. Nussenzweig,[4] and Junjie Chen[1]

[1]Division of Oncology Research, [2]Division of Immunology, and [3]Transplantation Biology, Mayo Clinic, Rochester, MN 55905
[4]Laboratory of Molecular Immunology, Howard Hughes Medical Institute, The Rockefeller University, New York, NY 10021
[5]Department of Microbiology and Immunology, University of Maryland School of Medicine, Baltimore, MD 21201
[6]Experimental Immunology Branch, National Cancer Institute, National Institutes of Health, Bethesda, MD 20892

53BP1 participates early in the DNA damage response and is involved in cell cycle checkpoint control. Moreover, the phenotype of mice and cells deficient in 53BP1 suggests a defect in DNA repair (Ward et al., 2003b). Therefore, we asked whether or not 53BP1 would be required for the efficient repair of DNA double strand breaks. Our data indicate that homologous recombination by gene conversion does not depend on 53BP1. Moreover, 53BP1-deficient mice support normal V(D)J recombination, indicating that 53BP1 is not required for "classic" nonhomologous end joining. However, class switch recombination is severely impaired in the absence of 53BP1, suggesting that 53BP1 facilitates DNA end joining in a way that is not required or redundant for the efficient closing of RAG-induced strand breaks. These findings are similar to those observed in mice or cells deficient in the tumor suppressors ATM and H2AX, further suggesting that the functions of ATM, H2AX, and 53BP1 are closely linked.

Introduction

Eukaryotic cells are constantly exposed to DNA-damaging agents. DNA double strand breaks (DSBs) are considered the most genotoxic form of DNA damage. They can arise endogenously from reactive oxygen intermediates or through exogenous exposure of cells to ionizing radiation (IR). DSBs can also be generated when DNA replication forks encounter DNA lesions, such as DNA single strand breaks or DNA cross-links (Khanna and Jackson, 2001). In addition, DNA DSBs occur as part of the normal development of the immune repertoire in B and T lymphocytes. During the process of V(D)J recombination, the recombination-activating gene proteins RAG1 and RAG2 introduce DSBs between observed recombination signal sequences and flanking V, D, or J coding segments of the antigen-combining sites of immunoglobulin and T cell receptor (TCR) genes (Gellert, 2002). A second type of DNA recombination, class switch recombination (CSR), also involves the generation of DNA DSBs. Stimulated mature B cells replace the heavy chain constant region of the initially expressed IgM antibodies with a different constant region. This isotype switching allows antibodies to change their effector functions while maintaining their antigen specificity (Honjo et al., 2002).

Improper processing of DSBs gives rise to chromosomal instability that can result in carcinogenesis. To maintain genomic integrity, eukaryotic cells have evolved different pathways for the repair of DNA DSBs. In the yeast *Saccharomyces cerevisiae*, DSBs seem to be repaired almost exclusively through high fidelity homologous recombination (HR), a process that uses the undamaged sister chromatid or homologous chromosome as a DNA template (Lin et al., 1999; Khanna and Jackson, 2001). In mammalian cells, nonhomologous end joining (NHEJ), which is the error-prone joining of DNA ends without the requirement for sequence homology, plays an important role in DSB repair, especially during the G1 phase of the cell cycle when no sister chromatid is available (Hendrickson, 1997; Khanna and Jackson, 2001).

53BP1 participates early in the DNA damage response. It rapidly localizes to sites of DNA strand breaks in response to IR and interacts with phosphorylated histone H2AX (γ-H2AX; Schultz et al., 2000; Xia et al., 2000; Anderson et al., 2001; Rappold et al., 2001; Abraham, 2002). Studies using siRNA directed against 53BP1 implicate a role of 53BP1 in checkpoint control (DiTullio et al., 2002; Fernandez-Capetillo et al., 2002; Wang et al., 2002). Notably,

Address correspondence to Junjie Chen, 1306 Guggenheim, Mayo Clinic, 200 First St., SW, Rochester, MN 55905. Tel.: (507) 538-1545. Fax: (507) 284-3906. email: Chen.junjie@mayo.edu

Key words: NHEJ; ATM; H2AX; V(D)J recombination; DNA repair

Abbreviations used in this paper: CSR, class switch recombination; DSB, double strand break; HR, homologous recombination; I, intronic; IR, ionizing radiation; NHEJ, nonhomologous end joining; PFGE, pulse field gel electrophoresis; TCR, T cell receptor.

53BP1-deficient mice are hypersensitive to IR and exhibit an increased predisposition for T cell lymphomas. Moreover, lack of 53BP1 protein is accompanied by immunodeficiency and increased chromosomal instability (Morales et al., 2003; Ward et al., 2003b). This phenotype is reminiscent of the phenotype observed in mice with a defect in the NHEJ pathway.

Therefore, we examined if 53BP1 plays a role in DNA DSB repair. Our results indicate that HR by gene conversion does not require 53BP1. Moreover, NHEJ-dependent V(D)J recombination is not affected in the absence of 53BP1, but CSR is severely impaired in 53BP1$^{-/-}$ mice. These results suggest that 53BP1 facilitates DNA end joining in a way that is not essential for V(D)J recombination.

Results and discussion

Role of 53BP1 in DNA repair

We have shown earlier that 53BP1$^{-/-}$ mice are hypersensitive to radiation and die within 2 wk after exposure to 8 Gy of IR (Ward et al., 2003b). Similarly, thymocytes isolated from irradiated 53BP1-deficient mice show a 2.11 ± 0.79-fold higher rate of apoptosis when compared with thymocytes isolated from irradiated wild-type littermates (Fig. 1 A). No significant difference in apoptosis was found in thymi of un-irradiated animals (unpublished data). Moreover, primary mouse embryonic fibroblasts derived from 53BP1$^{-/-}$ embryos exhibit a delayed exit from the G_2 phase of the cell cycle after radiation compared with wild-type mouse embryonic fibroblasts, presumably extending the time available for repair before entry into mitosis (Ward et al., 2003b). This radiation-induced G_2 delay is also observed in 53BP1$^{-/-}$ embryonic cells derived from 53BP1$^{-/-}$ blastocysts (unpublished data). This evidence suggests a possible repair defect in 53BP1$^{-/-}$ cells.

To examine whether or not the rejoining of DNA DSBs depends on 53BP1, we used the embryonic 53BP1$^{+/+}$ and 53BP1$^{-/-}$ cell lines to perform pulse field gel electrophoresis (PFGE) assays. As shown in Fig. 1 B, neither DNA DSB induction nor DSB rejoining appeared to be defective in 53BP1-deficient cells. The majority of DNA DSBs was rejoined within 15 min after exposure of cells to 10 or 20 Gy of IR, or within 24 h after exposure to 80 Gy of IR. Because the sensitivity of the PFGE assay may not be sufficient to detect subtle defects in DNA DSB repair, we performed additional assays to assess whether or not 53BP1 plays a role in HR or NHEJ, the two major DNA DSB repair pathways.

53BP1 is not required for HR

To test if 53BP1 is involved in HR, we used the recombination repair substrate DR-GFP designed to model HR-directed repair by using a tandem GFP repeat. The first GFP gene is inactivated by the introduction of an I-SceI recognition site, while the adjacent GFP gene is differentially mutated. After the introduction of a DSB at the I-SceI site, the GFP gene can be reconstituted by HR using the downstream inactivated GFP gene as a template.

We transfected 53BP1$^{+/+}$ or 53BP1$^{-/-}$ cells with DR-GFP and an I-SceI expression plasmid (pCBASce) and analyzed GFP expression 48 h later by flow cytometry. As a control, cells were transfected with DR-GFP alone or with a plasmid expressing an intact GFP gene. Although GFP-positive cells were very rare in both the wild-type (0.03–0.06%) and 53BP1-deficient cells (0.02–0.08%) transfected with DR-GFP alone (Fig. 2), an average of 4.80 ± 0.22% of 53BP1$^{+/+}$ cells and 4.21 ± 1.42% of 53BP1$^{-/-}$ cells expressed GFP 48 h after cotransfection with the I-SceI expression vector (Fig. 2). Similar numbers of GFP-positive cells were also observed after transfection of 53BP1$^{+/+}$ and 53BP1$^{-/-}$ cells with an intact control GFP expression vector, indicating that the transfection efficiency did not differ between 53BP1$^{+/+}$ and 53BP1$^{-/-}$ cells (Fig. 2). Thus, our

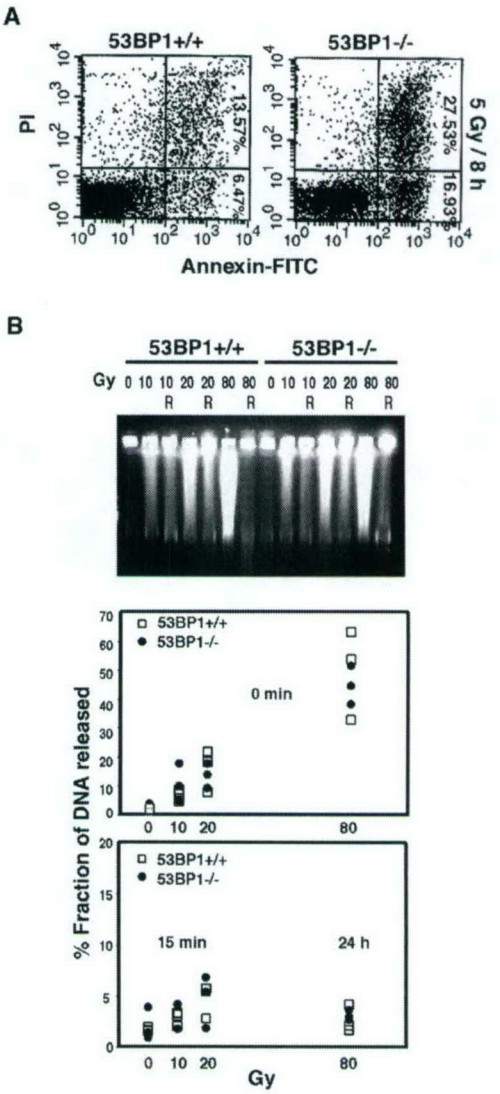

Figure 1. **53BP1 and DNA damage repair.** (A) Increased apoptosis in thymocytes derived from irradiated 53BP1$^{-/-}$ mice. Thymocytes were isolated from wild-type and 53BP1-deficient mice 8 h after irradiation with 5 Gy of IR and stained with annexin–FITC and PI. (B) 53BP1$^{-/-}$ embryonic cells show normal levels of DNA DSB rejoining. Wild-type and 53BP1-deficient cells were irradiated with different doses of IR and either allowed to recover (R) for 15 min or 24 h, as indicated, or immediately processed for PFGE analysis.

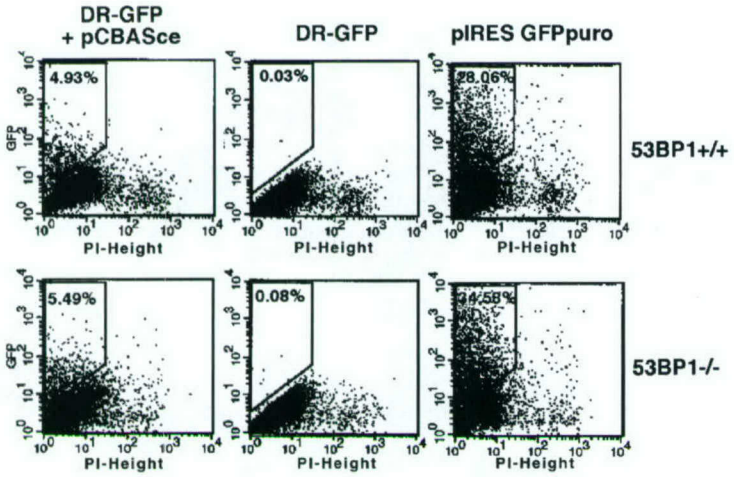

Figure 2. **53BP1 is not required for homology-directed repair.** Wild-type or 53BP1-deficient embryonic cells were cotransfected with an I-SceI repair substrate (DR-GFP) composed of two differentially mutated GFP and an I-SceI expression plasmid (pCBASce). Reconstitution of the GFP reporter gene by HR was assessed 46 h later by flow cytometry. As a control, cells were transfected with either DR-GFP alone or with a functional GFP expression plasmid (pIRES GFPpuro).

results suggest that DSB repair by gene conversion is not impaired in 53BP1-deficient cells.

53BP1 is not required for "classic" NHEJ and V(D)J recombination

Cells with a defect in the classic NHEJ pathway tend to use microhomologies near the DNA ends to promote end-joining reactions. To determine the relative efficiency of classic versus microhomology-directed NHEJ, we transiently transfected cells with a linearized plasmid substrate designed to create a BstX1 restriction site when joined by microhomology (Verkaik et al., 2002). Whereas plasmids recovered from DNA-PKcs–deficient cells indicated high levels of microhomology-directed joining, as previously described (Verkaik et al., 2002), direct end joining dominated in 53BP1-deficient cells as well as in wild-type or DNA-PKcs–reconstituted cells (Fig. 3), suggesting that 53BP1$^{-/-}$ cells have no major defect in NHEJ.

Another good indicator of NHEJ proficiency is V(D)J recombination. RAG-initiated site-specific V(D)J recombination is impaired in NHEJ-deficient cells and mice (Bassing et al., 2002). Notably, 53BP1$^{-/-}$ mice have up to a 50% reduction in the number of thymocytes and mature T cells compared with wild-type littermates (Ward et al., 2003b), a phenotype that could arise from impaired TCR V(D)J rearrangement. Therefore, we analyzed the rearrangement of different TCR loci in 53BP1$^{-/-}$ and 53BP1$^{+/+}$ mice. Overall, the level of V(D)J coding formation and the levels of TCRα excised signal joints appeared very similar in wild-type and knockout animals (Fig. 4). Quantitative analysis of the data confirmed that the level of the various TCR gene rearrangements tested did not differ between 53BP1$^{+/+}$ and 53BP1$^{-/-}$ mice (unpublished data). Together, our data indicate that 53BP1 is not essential for V(D)J recombination.

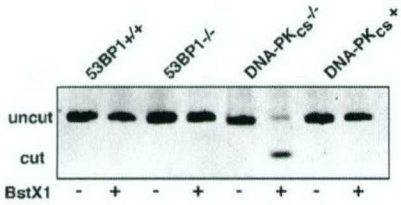

Figure 3. **53BP1 is not required for NHEJ.** Wild-type or 53BP1-deficient embryonic cells as well as DNA-PKcs–deficient and –reconstituted cells were transfected with plasmid pDVG94 linearized in such a way that joining on a particular microhomology creates a novel BstXI restriction site. 48 h later, the plasmid was recovered from the cells and the joining region was amplified by PCR. An aliquot of the PCR reaction was digested with BstXI, and uncut (180 bp) or BstXI-cut (120 bp) fragments were separated by gel electrophoresis.

53BP1 is required for efficient CSR

Unlike V(D)J recombination, the initiating factors and the mechanisms leading to the joining of DNA ends in CSR are only partially understood. Recent evidence suggests that CSR is triggered by AID (activation-induced deaminase)-induced deamination of cytosine residues in single strand DNA exposed by transcription of the immunoglobulin switch region. Excision of the resulting dU/dG mismatches on complementary DNA strands is thought to introduce DSBs (Muramatsu et al., 2000; Honjo et al., 2002; Petersen-Mahrt et al., 2002; Chaudhuri et al., 2003; Dickerson et al., 2003; Ramiro et al., 2003). Comparison of switch junction sequences indicates that switch recombination does not depend on either sequence-specific or HR mechanisms (Dunnick et al., 1993). Some evidence points to the NHEJ pathway because Ku-deficient B-cells show almost no detectable CSR (Casellas et al., 1998; Manis et al., 1998; Reina-San-Martin et al., 2003), and CSR to most constant region genes is severely impaired in DNA-PK–deficient B cells (Manis et al., 2002). To determine whether or not CSR is impaired in the absence of 53BP1, we stimulated wild-type and 53BP1$^{-/-}$ B cells to undergo switching to IgG1 in vitro with LPS and IL-4. Cells were also labeled with CFSE to track cell divisions by flow cytometry. CFSE dye dilution histograms were similar between 53BP1$^{-/-}$ and wild-type B cells, and no proliferation defects or increased mortality were observed (Fig. 5 A). Despite equivalent proliferation, the percentage of IgG1 positive cells after 96 h of incubation was 30% in wild-type cells but only 2% in 53BP1$^{-/-}$ B cells (Fig. 5 B), suggesting severely impaired CSR in the absence of 53BP1.

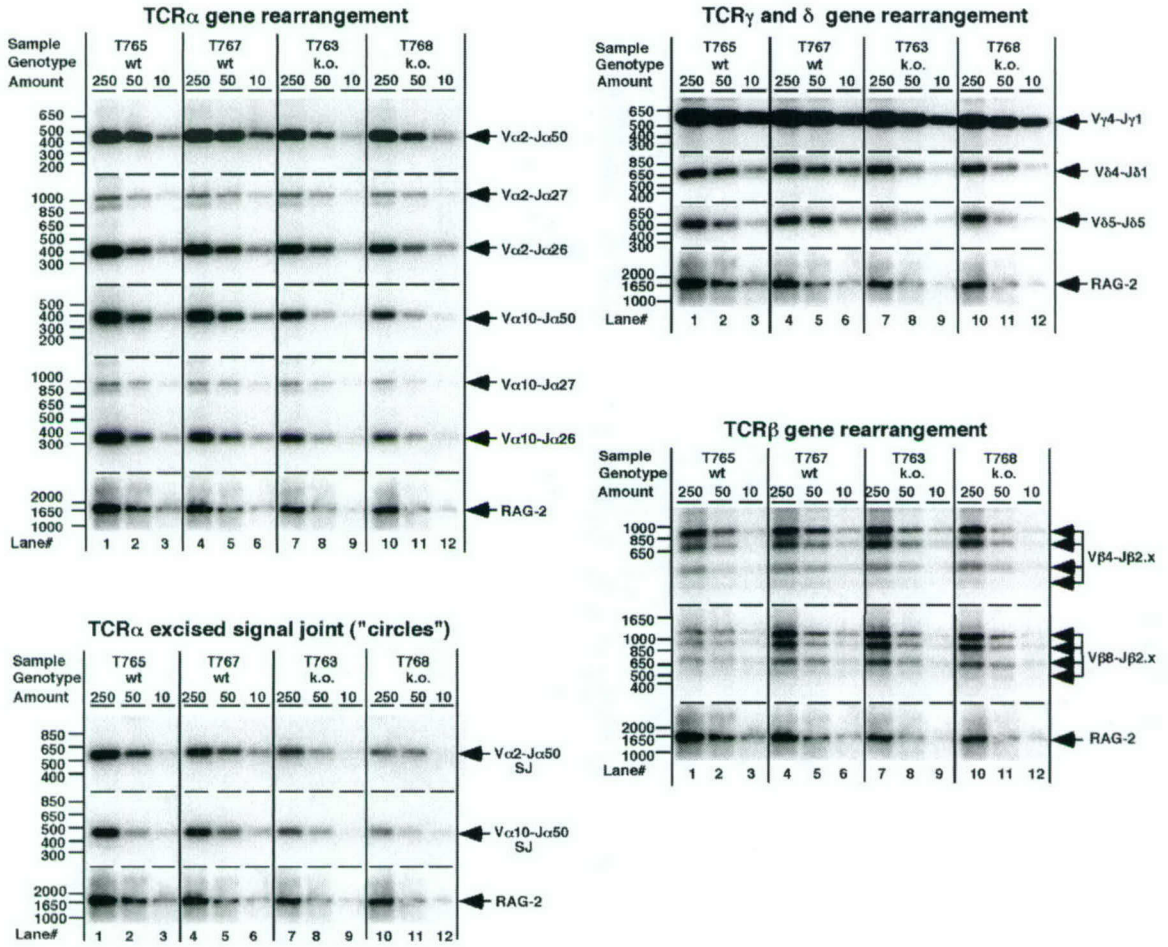

Figure 4. **Normal TCR gene rearrangements in the absence of 53BP1.** Serial dilutions of thymus DNA from 1-mo-old 53BP1-deficient mice and their wild-type littermates were PCR-amplified with primers specific for various TCRα, β, γ, or δ rearrangements or TCRα signal joints. The PCR products were Southern blotted and hybridized with the different gene-specific reverse probes as described in Materials and methods. PCR of the nonrearranging gene RAG-2 served as control for DNA quantity and integrity.

CSR is dependent on the rate of switch region transcription, and recombination is targeted to individual switch regions by transcription from intronic (I) promoters located upstream of each switch region. To determine if sterile transcription is normal in 53BP1$^{-/-}$ B cells, we measured the relative amounts of the μ and γ1 preswitch sterile transcripts (Reina-San-Martin et al., 2003) by quantitative real-time RT-PCR. As shown in Fig. 5 C, μ and γ1 sterile transcripts were expressed at comparable levels in wild-type and 53BP1$^{-/-}$ B cells, suggesting that sterile transcription of the IgM and IgG1 switch regions is not altered in the absence of 53BP1.

CSR is a deletional recombination reaction that results in the looping out and deletion of intervening DNA sequences as a circular episome (Iwasato et al., 1990; Matsuoka et al., 1990; von Schwedler et al., 1990). The looped-out circular DNA contains segments of Sμ and the target S region, including its I promoter. This promoter is still active in the looped-out circle and drives the synthesis of the circle transcript, a hybrid containing the I and Cμ exons (Kinoshita et al., 2001). The circle transcript appears only after productive CSR, and its level is proportional to the frequency of successful joining events (Kinoshita et al., 2001). To determine if 53BP1 deficiency has an impact on the frequency of joining during CSR, we used real-time RT-PCR to quantitate γ1 circle transcripts in B cells stimulated with LPS and IL-4. The level of γ1 circle transcript in 53BP1$^{-/-}$ B cells was 6.6-fold reduced when compared with wild-type (Fig. 5 D) and is consistent with decreased CSR in the absence of 53BP1 (Fig. 5 B). Together, these data indicate that 53BP1 is required for CSR at the DNA level and that impaired CSR in 53BP1$^{-/-}$ B cells is not due to abnormal B cell proliferation.

The impairment in CSR observed in 53BP1-deficient cells is less severe than the CSR defects in B cells deficient for components of the NHEJ pathway (Casellas et al., 1998; Manis et al., 1998, 2002). However, it appears to be more severe than the defect described in H2AX-deficient mice (Celeste et al., 2002; Reina-San-Martin et al., 2003). Moreover, the fact that 53BP1-null mice, like H2AX-deficient mice, support normal V(D)J recombination implies that the joining of class switch junctions differs from the rejoining of RAG-induced strand breaks. The repair pathways could be

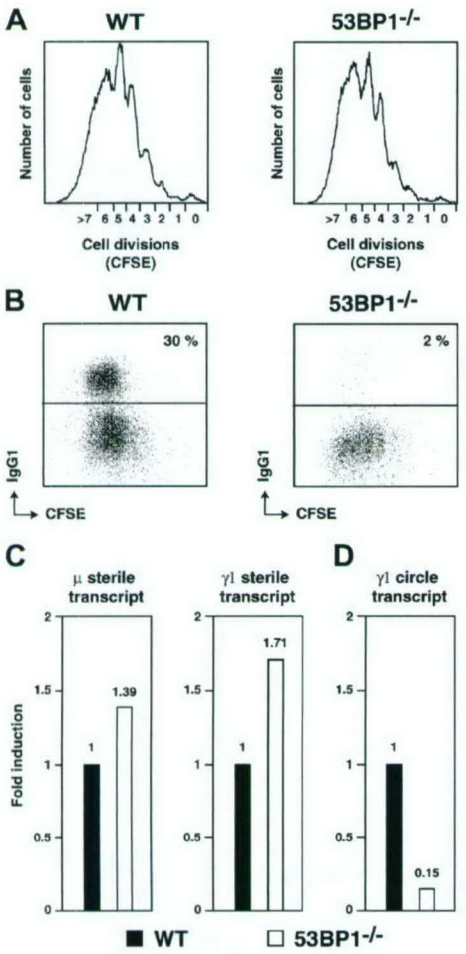

Figure 5. **CSR is dependent on 53BP1.** Cell division (A) and surface IgG1 expression (B) as measured by flow cytometry on live CFSE-labeled wild type (WT) and 53BP1$^{-/-}$ B cells stimulated with LPS plus IL-4 for 4 d. Results are representative of four experiments. Real-time RT-PCR for μ and γ1 sterile transcripts (C) and γ1 circle transcript (D) in wild-type (solid bars) and 53BP1$^{-/-}$ (open bars) B cells stimulated with LPS and IL-4 for 3 d. Results from four independent cultures are expressed as fold induction relative to wild-type B cells.

different for V(D)J recombination and CSR. Alternatively, 53BP1 and H2AX could be indirectly involved in the repair process by facilitating chromosomal accessibility or influencing chromatin organization and the loading of repair proteins. Because RAG proteins bind directly to DNA ends during V(D)J recombination, the involvement of RAG proteins may alleviate the requirement of a structural role of H2AX and 53BP1 in V(D)J recombination. Of course, it is also possible that the role of 53BP1 or H2AX in chromatin alterations is specific to CSR. Further analysis of H2AX and 53BP1 in the regulation of chromatin structure will be necessary to test these hypotheses.

Both 53BP1 and H2AX become rapidly phosphorylated by ATM (ataxia telangiectasia mutated) after IR and interact with each other at sites of DNA breaks (Burma et al., 2001; Rappold et al., 2001; Ward et al., 2003a). Similar to H2AX- or 53BP1-deficient cells, ATM-deficient cells also display a defect in CSR but support normal V(D)J recombination (Pan-Hammarstrom et al., 2003), suggesting that the functions of these proteins are closely linked. Although the exact role of 53BP1, ATM, and H2AX in DNA DSB repair remains to be determined, all three proteins appear to function in facilitating certain aspects of DNA end joining. Unraveling their mode of action in DNA repair will be a step further in our understanding of the process of carcinogenesis.

Materials and methods

Cell lines

53BP1-deficient and 53BP1 wild-type embryonic cell lines were established from day 3 blastocysts by a standard procedure. DNA-PKcs–deficient cells (V3.3) and DNA-PKcs reconstituted cells (V3.155) were a gift of D.C. Chen, Lawrence Berkeley National Laboratory, Berkeley, CA.

Apoptosis assay

To assess apoptosis in irradiated thymocytes, 6-wk-old 53BP1$^{-/-}$ mice and wild-type littermates were exposed to 5 Gy of IR. 8 h later, the animals were killed and the thymocytes were isolated and stained with annexin-FITC (Molecular Probes) and PI before analysis on a FACScan.

PFGE assay

For determination of DSB rejoining, equal numbers of exponentially growing cells labeled with [^{14}C]thymidine were exposed to IR at the indicated doses. After various recovery times, the cells were embedded in agarose plugs and lysed for 16 h in 1% sarcosyl, 0.5 M EDTA, and 1mg/ml proteinase K. For determination of break induction, cells were embedded in plugs before irradiation and lysed immediately. The plugs were washed in TE buffer and electrophoresis was performed in a CHEF DRII system (Bio-Rad Laboratories) for 65 h in 0.8% agarose in 0.5× TBE at 14°C with a field strength of 1.5 V/cm and pulse times increasing from 50 to 5,000 s. For quantification, single lanes were cut into ~1-cm-thick slices, melted, and analyzed on a scintillation counter. The level of DNA breakage was estimated by the fraction of activity released from the plug into the gel.

HR repair assay

The efficiency of HR was assessed using an I-SceI repair substrate (DR-GFP) composed of two differentially mutated GFP and an I-SceI expression plasmid (pCBASce; both gifts from M. Jasin, Memorial Sloan-Kettering Cancer Center and Cornell University Graduate School of Medical Sciences, New York, NY). 53BP1$^{+/+}$ and 53BP1$^{-/-}$ embryonic cells were transfected by electroporation with either 5 μg DR-GFP plus 5 μg pCBA-Sce or 5 μg DR-GFP alone. In addition, an aliquot of the cells was transfected with a functional GFP expression plasmid (pIRES-GFP Puro) to monitor transfection efficiency. 46 h later, cells were harvested and GFP expression was assessed by flow cytometry.

NHEJ repair and V(D)J assays

The assay for microhomology-directed end joining was performed as described previously (Verkaik et al., 2002). 5 μg of blunt-ended linear pDVH94 plasmid (a gift from D.C. van Gent, Erasmus Medical Center, Rotterdam, Netherlands) was electroporated into 4 × 10^6 cells, and extrachromosomal DNA was isolated 48 h later. DNA end-joining regions were amplified by PCR, and microhomology-directed end joining was assessed by BstXI restriction digestion.

V(D)J recombination in vivo was tested by a semiquantitative PCR method as described previously (Livak et al., 1995, 1999; Livak and Schatz, 1996).

Primer sequences not published before are as follows: Vβ4, 5′ GAAGCCTCTAGAGTTCATGTTTTC 3′; Jβ2.5, 5′ GAGCCGAGTGCCTGGCCCAAAGTA 3′; Vα2, 5′ GCCGGATCCAGGAGAAACGTGACCAGCAG 3′; Vα10, 5′ AGCGAATTCCCGCGTCCTTGGTTCTGCA 3′; Vα2 signal joint, 5′ CTCTGGATCCGAATTCATYTAAACTAGTTAA 3′, where Y = C or T; Vα10 signal joint, 5′ CCTGGATCCAGAATTCTACCAATACARGAAAG 3′, where R = A or G; and Jα26/27, 5′ CCTGGATCCTTACTGTCATATATCGAA 3′.

Lymphocyte cultures and flow cytometry

Resting B lymphocytes were isolated from the spleen using CD43 microbeads (Miltenyi Biotec), labeled with CFDA-SE for 10 min at 37°C (5 μM; Molecular Probes), and cultured (10^6 cells/ml) with LPS (25 ng/ml; Sigma-

Aldrich) and IL-4 (5 ng/ml; Sigma-Aldrich) for 4 d. Percentage of switching to IgG1 was determined by flow cytometry by using Biotin-anti-IgG1 (BD Biosciences) and Streptavidin-PE-Cy7 (Caltag). Dead cells were excluded from the analysis by staining with Topro-3 (Molecular Probes).

Quantitative real-time RT-PCR

Total RNA was extracted with TRIzol (Invitrogen) and reverse transcribed with random hexamers and superscript II reverse transcriptase (Invitrogen). First strand cDNA was used for SYBR green fluorogenic dye real-time PCR (Applied Biosystems). Primers used and PCR conditions are described in Reina-San-Martin et al. (2003).

We thank David C. Chen, Maria Jasin, and Dik C. van Gent for valuable reagents. We are grateful to Larry Karnitz, Scott Kaufmann, and members of the Chen laboratory for helpful discussions.

This work was supported by a grant from the National Institutes of Health to J. Chen (CA100109). J. Chen is a recipient of a Department of Defense (DOD) breast cancer career development award (DAMD17-02-1-0472). I. Ward is supported by a postdoctoral fellowship from the DOD Breast Cancer Research Program (DAMD17-01-1-0317).

Submitted: 2 March 2004
Accepted: 2 April 2004

References

Abraham, R.T. 2002. Checkpoint signalling: focusing on 53BP1. *Nat. Cell Biol.* 4:E277–E279.

Anderson, L., C. Henderson, and Y. Adachi. 2001. Phosphorylation and rapid relocalization of 53BP1 to nuclear foci upon DNA damage. *Mol. Cell. Biol.* 21:1719–1729.

Bassing, C.H., W. Swat, and F.W. Alt. 2002. The mechanism and regulation of chromosomal V(D)J recombination. *Cell.* 109:S45–S55.

Burma, S., B.P. Chen, M. Murphy, A. Kurimasa, and D.J. Chen. 2001. ATM phosphorylates histone H2AX in response to DNA double-strand breaks. *J. Biol. Chem.* 276:42462–42467.

Casellas, R., A. Nussenzweig, R. Wuerffel, R. Pelanda, A. Reichlin, H. Suh, X.F. Qin, E. Besmer, A. Kenter, K. Rajewsky, and M.C. Nussenzweig. 1998. Ku80 is required for immunoglobulin isotype switching. *EMBO J.* 17: 2404–2411.

Celeste, A., S. Petersen, P.J. Romanienko, O. Fernandez-Capetillo, H.T. Chen, O.A. Sedelnikova, B. Reina-San-Martin, V. Coppola, E. Meffre, M.J. Difilippantonio, et al. 2002. Genomic instability in mice lacking histone H2AX. *Science.* 296:922–927.

Chaudhuri, J., M. Tian, C. Khuong, K. Chua, E. Pinaud, and F.W. Alt. 2003. Transcription-targeted DNA deamination by the AID antibody diversification enzyme. *Nature.* 422:726–730.

Dickerson, S.K., E. Market, E. Besmer, and F.N. Papavasiliou. 2003. AID mediates hypermutation by deaminating single stranded DNA. *J. Exp. Med.* 197: 1291–1296.

DiTullio, R.A., T.A. Mochan, M. Venere, J. Bartkova, M. Sehested, J. Bartek, and T.D. Halazonetis. 2002. 53BP1 functions in an ATM-dependent checkpoint pathway that is constitutively activated in human cancer. *Nat. Cell Biol.* 4:998–1002.

Dunnick, W., G.Z. Hertz, L. Scappino, and C. Gritzmacher. 1993. DNA sequences at immunoglobulin switch region recombination sites. *Nucleic Acids Res.* 21:365–372.

Fernandez-Capetillo, O., H.T. Chen, A. Celeste, I. Ward, P.J. Romanienko, J.C. Morales, K. Naka, Z. Xia, R.D. Camerini-Otero, N. Motoyama, et al. 2002. DNA damage-induced G(2)-M checkpoint activation by histone H2AX and 53BP1. *Nat. Cell Biol.* 4:993–997.

Gellert, M. 2002. V(D)J recombination: RAG proteins, repair factors, and regulation. *Annu. Rev. Biochem.* 71:101–132.

Hendrickson, E.A. 1997. Cell-cycle regulation of mammalian DNA double-strand-break repair. *Am. J. Hum. Genet.* 61:795–800.

Honjo, T., K. Kinoshita, and M. Muramatsu. 2002. Molecular mechanism of class switch recombination: linkage with somatic hypermutation. *Annu. Rev. Immunol.* 20:165–196.

Iwasato, T., A. Shimizu, T. Honjo, and H. Yamagishi. 1990. Circular DNA is excised by immunoglobulin class switch recombination. *Cell.* 62:143–149.

Khanna, K.K., and S.P. Jackson. 2001. DNA double-strand breaks: signaling, repair and the cancer connection. *Nat. Genet.* 27:247–254.

Kinoshita, K., M. Harigai, S. Fagarasan, M. Muramatsu, and T. Honjo. 2001. A hallmark of active class switch recombination: transcripts directed by I promoters on looped-out circular DNAs. *Proc. Natl. Acad. Sci. USA.* 98:12620–12623.

Lin, Y., T. Lukacsovich, and A.S. Waldman. 1999. Multiple pathways for repair of DNA double-strand breaks in mammalian chromosomes. *Mol. Cell. Biol.* 19:8353–8360.

Livak, F., and D.G. Schatz. 1996. T-cell receptor alpha locus V(D)J recombination by-products are abundant in thymocytes and mature T cells. *Mol. Cell. Biol.* 16:609–618.

Livak, F., H.T. Petrie, I.N. Crispe, and D.G. Schatz. 1995. In-frame TCR delta gene rearrangements play a critical role in the alpha beta/gamma delta T cell lineage decision. *Immunity.* 2:617–627.

Livak, F., M. Tourigny, D.G. Schatz, and H.T. Petrie. 1999. Characterization of TCR gene rearrangements during adult murine T cell development. *J. Immunol.* 162:2575–2580.

Manis, J.P., Y. Gu, R. Lansford, E. Sonoda, R. Ferrini, L. Davidson, K. Rajewsky, and F.W. Alt. 1998. Ku70 is required for late B cell development and immunoglobulin heavy chain class switching. *J. Exp. Med.* 187:2081–2089.

Manis, J.P., D. Dudley, L. Kaylor, and F.W. Alt. 2002. IgH class switch recombination to IgG1 in DNA-PKcs-deficient B cells. *Immunity.* 16:607–617.

Matsuoka, M., K. Yoshida, T. Maeda, S. Usuda, and H. Sakano. 1990. Switch circular DNA formed in cytokine-treated mouse splenocytes: evidence for intramolecular DNA deletion in immunoglobulin class switching. *Cell.* 62: 135–142.

Morales, J.C., Z. Xia, T. Lu, M.B. Aldrich, B. Wang, C. Rosales, R.E. Kellems, W.N. Hittelman, S.J. Elledge, and P.B. Carpenter. 2003. Role for the BRCA1 C-terminal repeats (BRCT) protein 53BP1 in maintaining genomic stability. *J. Biol. Chem.* 278:14971–14977.

Muramatsu, M., K. Kinoshita, S. Fagarasan, S. Yamada, Y. Shinkai, and T. Honjo. 2000. Class switch recombination and hypermutation require activation-induced cytidine deaminase (AID), a potential RNA editing enzyme. *Cell.* 102:553–563.

Pan-Hammarstrom, Q., S. Dai, Y. Zhao, I.F. van Dijk-Hard, R.A. Gatti, A.L. Borresen-Dale, and L. Hammarstrom. 2003. ATM is not required in somatic hypermutation of VH, but is involved in the introduction of mutations in the switch mu region. *J. Immunol.* 170:3707–3716.

Petersen-Mahrt, S.K., R.S. Harris, and M.S. Neuberger. 2002. AID mutates *E. coli* suggesting a DNA deamination mechanism for antibody diversification. *Nature.* 418:99–103.

Ramiro, A.R., P. Stavropoulos, M. Jankovic, and M.C. Nussenzweig. 2003. Transcription enhances AID-mediated cytidine deamination by exposing single-stranded DNA on the nontemplate strand. *Nat. Immunol.* 4:452–456.

Rappold, I., K. Iwabuchi, T. Date, and J. Chen. 2001. Tumor suppressor p53 binding protein 1 (53BP1) is involved in DNA damage–signaling pathways. *J. Cell Biol.* 153:613–620.

Reina-San-Martin, B., S. Difilippantonio, L. Hanitsch, R.F. Masilamani, A. Nussenzweig, and M.C. Nussenzweig. 2003. H2AX is required for recombination between immunoglobulin switch regions but not for intra-switch region recombination or somatic hypermutation. *J. Exp. Med.* 197:1767–1778.

Schultz, L.B., N.H. Chehab, A. Malikzay, and T.D. Halazonetis. 2000. p53 binding protein 1 (53BP1) is an early participant in the cellular response to DNA double-strand breaks. *J. Cell Biol.* 151:1381–1390.

Verkaik, N.S., R.E. Esveldt-van Lange, D. van Heemst, H.T. Bruggenwirth, J.H. Hoeijmakers, M.Z. Zdzienicka, and D.C. van Gent. 2002. Different types of V(D)J recombination and end-joining defects in DNA double-strand break repair mutant mammalian cells. *Eur. J. Immunol.* 32:701–709.

von Schwedler, U., H.M. Jack, and M. Wabl. 1990. Circular DNA is a product of the immunoglobulin class switch rearrangement. *Nature.* 345:452–456.

Wang, B., S. Matsuoka, P.B. Carpenter, and S.J. Elledge. 2002. 53BP1, a mediator of the DNA damage checkpoint. *Science.* 298:1435–1438.

Ward, I.M., K. Minn, K.G. Jorda, and J. Chen. 2003a. Accumulation of checkpoint protein 53BP1 at DNA breaks involves its binding to phosphorylated histone H2AX. *J. Biol. Chem.* 278:19579–19582.

Ward, I.M., K. Minn, J. Van Deursen, and J. Chen. 2003b. p53 Binding protein 53BP1 is required for DNA damage responses and tumor suppression in mice. *Mol. Cell. Biol.* 23:2556–2563.

Xia, Z., J.C. Morales, W.G. Dunphy, and P.B. Carpenter. 2000. Negative cell cycle regulation and DNA damage-inducible phosphorylation of the BRCT protein 53BP1. *J. Biol. Chem.* 276:2708–2718.